

Supporting Information for

TapA acts as specific chaperone in TasA filament formation by strand complementation

Yvette Roske, Florian Lindemann, Anne Diehl, Nils Cremer, Victoria A. Higman, Brigitte Schlegel, Martina Leidert, Kristina Driller, Kürşad Turgay, Peter Schmieder, Udo Heinemann, Hartmut Oschkinat*

*Corresponding Author: Hartmut Oschkinat
Email: oschkinat@fmp-berlin.de

This PDF file includes:

Figures S1 to S14
Tables S1 to S8
SI References

Supplementary Figures

- 1 **TasA** *B. subtilis* (strain 168)|P54507
- 2 **CalY1** *B. cereus* (clone B905)|A0A0A3VY99
- 3 **CalY2** *B. cereus* (clone B905)|A0A0E3SV09
- 4 **Thermococcus gorgonarius**|A0A2Z2M7U5
- 5 **Bacillus mycoides**|C2Q5K3
- 6 **Bacillus thuringiensis**|K0G0I4
- 7 **Haloferax gibbonsii**|A0A871BKPO
- 8 **Paenibacillus graminis**|A0A089M0B1
- 9 **Aquisalibacillus elongatus**|A0A3N5B9I6
- 10 **Bacillus oleivorans**|A0A285CS81
- 11 **Aureibacillus halotolerans**|A0A4R6UFZ6
- 12 **Bacillus sp. 1NLA3E|N0ATI4**
- 13 **Blautia luti**|A0A564VQ52
- 14 **Bacillus oleivorans**|A0A285CTH3
- 15 **Paenibacillus taihuensis**|A0A3D9SB88
- 16 **Neobacillus mesonae**|A0A3T0I131
- 17 **Methanosarcina barkeri**|A0A0G3CB53
- 18 **Lachnospiraceae bacterium**|A0A7G9BU6
- 19 **Virgibacillus salinus**|A0A1H1GBR8
- 20 **Sporosarcina sp. resist**|A0A7G8X4J2
- 21 **Neobac. massiliamazoniensis**|A0A0U1NYG4
- 22 **Piscibacillus halophilus**|A0A1H9E238
- 23 **Hungateella hathewayi**|A0A174ECC6
- 24 **Alteribac. persepolensis**|A0A1G8JRA6
- 25 **Bacillus velezensis**|A0A8F9SKQ0
- 26 **Psychrobacillus sp. OK028**|A0A1G9SR36
- 27 **Bacillus pillulus**|A0A8G1J983
- 28 **Haloechinotrix alba**|A0A238Y1I1
- 29 **Clostridium cf. saccharolyticum**|D6DLJ6
- 30 **Salimicrobium halophilum**|A0A1G8SB90
- 31 **Bacterium BMS3Abin01**|A0A2H6K5U5

29 42 62
MGMKKLSLG.VASAAALGLALVGGTAAFFNDIKS.KDATFASGTLDL.S...AKENSASVN..LSNLKPGD.....
MSLKKKLMGM.VASAAALGLALVGGTAAFFSDKVEV.SNNTFAAGTLDLTLN.....PKTLVDTKDLKPGD.....
MTLKKKLMGM.ITSALVGAALVGGTAAFFSDKVEV.SNNTFAAGTLDLALN.....PSTVNVNSLNLKPGD.....
MKSIAVA.LLLZGLVFAAGYGTWAIYQDTESEGNISIELGTLDLVLDG.....VPVANGQWFPINAVSPGD.....
MINEEQKMSLKKKLVGV.VSAAALGLSLIGGGTYAFSDQVV.TNNSFAAGTLDLAMDQ.....PTSLNLLENLKPGD.....
MSLKQKVMGM.VWTATLGLSLTGGVFAFSDSET.SNSFQAAGTLDLSIN.....PSVIVDVKDLKPGD.....
MPEKVFKLRRRALGGLLTIGAGSAAAGTFFALFNDTESSSENTLQAQGLSLADG.....ASSASVADKLAGPGE.....
MGIKKTLPFG.IASAAALGLSLIGGGTYAFSDQAT.STATFAAGTLDLMSD.....PSVIVDQNLKPGD.....
MDIKKKLGM.VLGTAGLGLSLVGGTAAFFNDVEE.TTNVFAAGVLDLE.....IGESTHDFSLDNLKPGD.....
MSLKKKMSGM.ILSGALVSLIGGGTAAFFNDVEE.VNNTLAAGTLDLVL.....VGEENTMNFSLNLKPGD.....
MGLKRLKATS.VMSASLGLSLIGGGTAAFFNDVEN.IENTFAAGTLDLAVI.....TKDKNSVFK.LLNMKPGD.....
MSIKRKLGLG.AASAAALGLSLIGGGTYAFSDAAT.LHNGFAAGTLDLVELQ.....AWDFPLNFDLSNLKPGD.....
MMKNRKLKVG.I.ALAAVIT.ALAAGTAAALYDFET.ATNSFTVGVKVDIDL.....EPNMKPEDNTDLPVQ.....
MSLKKKLMGM.ALSATLGLSLVGGTAAFFNDIEE.VNASLAAGSLDLV.....VDEYGNPVFNISNLKPGD.....
MSIKKALGMG.IITASLGLSLIGGGTYAFNDAGSISQNSFASGTINLNATK.....AWDFANFDLNNKPGD.....
MGIKKLGLG.I.MALAGIATLAVLAGTAAFFQDTESTGTNTFSSGTLDMKLSNDGSTYDGTDTVTSFPAFPGD.....
MANKRVLVS.IASALGAVLAVLAGTAAFFQDTESTGTNTFSSGTLDMKLSNDGSTYDGTDTVTSFPAFPGD.....
MKRG..TKTI.MLAAALGAVLIVGGVSAFFTDADT.ATNTFTVGVKISLDLQ.....EPSWNPQDKVLTNPQ.....
MNIKKKMGTV.ILAGLGLSLVGGTAAFFNDVEE.IDNTFTAGTLDLVL.....LTGQETSFEFSNLKPGD.....
MGIKQKLMG.IIATGALVSLIGGGTYAFNDVEE.STNTFAAGTLDLSLK.....PETIDVKNKPGD.....
MKIKTKLGMV.AASGALGLALVGGTAAFFNSKVE.ATSTFEMGTLDLSVN.....PSTIVSVKLNKPGD.....
MSIKKALGMG.VLSAALGLSLIGGGTYAFSDTEE.TNNTFAAGTLDLSVD.....PTTVADGTLNPKPGD.....
MRRNYRKASQIVSALAVLIGGGTYAFNSQDLS.ASNVFLTKGYDLDLH.....EYFKPPGWDQVPG.....
MKKTKALQAL.IITAGGLVSLIGGGTYAFNSQDLS.TDGEITAGTLDLNDLS.....EYFKPPGWDQVPG.....
MGMKKLSLG.VASAAALGLALVGGTAAFFNDVKS.TDATFASGTLDL.S...AKEQASVN..LSNLKPGD.....
MSIKQKLMG.IITAGLGLSLVGGTAAFFNDVEE.MNSFAAGTLDLHIVAG.....ADNADNAINVTINMIPGD.....
MAKRSIRLG.VLSGALGLALVGGTAAFFNDVEE.ANAVYSTGELDL.S...AKENSASVN..LSNLKPGD.....
MRIEKKTAGV.VASAAALGLALVGGTAAFFNDVEE.IDNTFTAGTLDLVL.....LTGQETSFEFSNLKPGD.....
MKYKYLGMG.IIAGLGLSLVGGTAAFFNDVEE.IANPFTSNSAIDMT.....ENYPAEAGNLPGE.....
MSVKKLLAVG.VLMTAGLGLSLVGGTAAFFNDVAK.VNHFASGELNLE.V...GDSHKAISFDTLNMKPGD.....
MNRKILIS.VLMSLALMAGLAVGTYAFSDSETSGNSFAAGTLDLKVADNDE.GYDGGVQTVIWMIPGD.....

- 1 KLTKDFQFENNGSLA.IKEVLMALNYGD..FKA.....NGSNTSPEDFLSQFEVTLTVGKGGNGYKPNII.LDDANLKDLYLMSAKN..DAAAEEKIKKQIDPKFLNAGSKVNVATIDGKTAP
- 2 SVKKEFLQNSGLT.IKDVKLATK.YTVKDAKD.....NAGEDFGKHVKVFLNMDKQSE.....PYETTLADLQKVPDLAK.DTFAPEWG.....
- 3 TIEKFEKLEKNSLD.IKKVLLKTD.YNVEDKDKD.....NK.DDFGKHVKVFLNMDKQSE.....IVKQTLDKLKGDTLAVDN.DLSAWFHW.....
- 4 LYNGDIKINNGTVD.ADHVEIAIELVWEDDGNIDNGRAWGPEDEVNGVGLDQEIKNVMQYREEWIG.....PSATLQLENGAALGDVVYVNVNLPAPPRVNG
- 5 KILKKFNLNSGTL.IKDMMKID.YTVNLDLQK.....NTTEDFGKHVKVFLNMDKQSP.....VYETTLAEKLSQSPETASKKVYFYSKWET.....
- 6 FIEKNFTLEKNSLD.IKVALETS.YEVTDAKLN.....NDGEDLGHIIKVLVNDGKPSMNPDDHE.....ILWETKSLKMTKPEDVSTSLERHNLID.....
- 7 TDTFEVDLENDGTLDGLSDIDLAL.TENDSDATAGDD.....GDADASVADLAVGLDVTTFEVG.....S.DLVLADRFGSGLATLADVANNAGGED..DSD
- 8 TVTKTKFKKNDGTLD.IGSILLKTT.TEVTDTLGD.....NNGADLSKFKVKKFLKNNDKGTIISP.....EVVYETTLDAKLGQTPDLSN.TGWQJLLT.....
- 9 HWTETLVRNNGTLD.INQILT.SIEVTG.WEDVDALDLSKVVYDAGNKKLSDFLQFQEVTT.....DGDGNV.FFDGTLDLHGGQSNID.ITGT
- 10 YFNKSLVNLNSGSLD.INQILVHANKLAG.WTKDKVLDLNTIEIGANSNNSDEDFLQFQEVTT.....DGDGNV.FFDGTLDLHGGQSNID.ITGT
- 11 SKTAEFELKNSGLA.IKEVLLDITVPEDFGKNGEN..EYVNHGHEEAEIDLEQFQEVILRDEETG.....YDFTLIEEKO..GVTLADFAKIDLPAEIEVGDGANLAPIH.TERP
- 12 SFRQFVKNNSGLA.IEDVFMGVT.ANVTNPLGTG.....GTSQFDLALNKKYFVDTAPPYIDPDAPDA.....GYLLINSQDISLREAIAGDFG.KIKADYIKNG.KLNL
- 13 VIRKDPVYANKGVNE.AFVYLEVSVPVRNVIATAK.....DGRNMAKTELFSTFKNKDWTQL.....ERTEVQNMVYTYAYN.....HILKPGTKTTT
- 14 THRYIKLDNAGTLA.IKDVLLSIDSVN..FTDYL.P..VGADSDIYGANTADEVLSQFVTLTKTGEGEADIEISS.ADNITLADIVLATNPQDLDPVIAKLSAIG.NGHVWDGHNWLASAA..QN
- 15 VTRQFVNLNSGSLD.IANTLMSFT.....SDA.....GSDAGLNTLTSYFVSGNII.....N.....EYLLMNSQDITLSDAIAGNYAG.KIKAEYLTDGKLN
- 16 TVERTFDLKNVNSGLA.IEDTVLDFSKVSVENPLNTG.....ATDDDFLSALSVTYFYEVTVN..GQYVPE.....MLVNSQKLSKDAIAGNYAG.KIQPRFLKGT.KLNL
- 17 TFGNELRFTVNSVNI.INHLYMYPEDLNTSGGGTG.....IKLSDKIITKVTGHTIDRGSNLVWG.....NRADFVGSVNGRGTLLTEFCSAKFAVAYCLSPIIFG
- 18 VVQKDPQKNSGSLD.EFVLEVTVPYKNVTVND.....AGVQKTAADTELVKTYTVNAGWTELG.....SGEKDVAETVLRHYVGTDOACTALAKDQVTPA
- 19 SFTKTIITLKNNSGLA.IKEILMSMAIEGSIWIDKT..NQKLPDN.GMNTVDFLQFQEVTT.....QGETEYFNGTDFEALN.....KIVMGS
- 20 WNNRDFLKNNSGSLD.ISKVLKTE.YTVTKNDG.....NVENFGSHRNVNFMNHDKSIPTGPTGL.....DNVVYQTLAEIQMTPDAVEN.RFVYPLYE.....
- 21 YMTRSFVKNNSGSLA.IKDVLMGSAF.....ANTDGLKHRNVLFNQDKAALGTWLPE.....DQVVFQTLVLDLQNTPDAVEN.KYFHDLHE.....
- 22 VWRFEFLNSGTLD.ISSIDLSTA.YEVIDAEGN.....NTDDFGKHVKVFLNMDKQSE.....NDVIAETTLVLDLQNTPDAVENVQGFTHLLGL..NG
- 23 EIPKVKDIKNSGSLD.VAVARMTESVCRKEDVITTYETVD.GRKRTERQKVASQGVLPQFEDSDGTQEFALKNFG.....SDVVYAEAKSPEEYRNKVVYTYDENSKAYFYFIMGLIEGNTSPG
- 24 TEGENITVNTNSGSLD.EMVPLQLDVEIKDKKNDAS.....ETLSDEYMKMTFR.....NDNMWSEISADKVIDNDRGFPVDPSPD
- 25 KLTKDFEFLKNSGLA.IKEVLMALNFTD..FKG.....AKNGESAEDFLSQFEVTLTVGKGGNGYKPNII.LDANLKDLYLMSAKN..DAAAEEKIKKQIDPKFLNAGSKVNVATIDGKTAP
- 26 TMLRTFKLNTNSGSLD.VSKVLLTSK.YTVVDAKGS.....NGGADFGHEHKKVFLINKDKRTE.....VHETTLKDL.S.KTDVTR.DLSEGLITDQ.....KIVMGS
- 27 RKKEFHFNKNSGLA.INQVLMSLDYSQ..FDG.....ASAKNGKNTAEELFSQFQVSLTVGAEAGNGYKPNII.LDANLKDLYLMSAKN..DAAAEEKIKKQIDPKFLNAGSKVNVATIDGKTAP
- 28 GEGKTIQENNSGSLD.LTVDYSTDEVCNDPE.....IDAERAFYDESEIDECGN.....QGETEYFNGTDFEALN.....KIVMGS
- 29 TVEKEPYVNSGSLD.LVRLKMDTYIDQNGNRKD.....DLGAVYFGLQPEED.....VYTLVLDGDDDDVQVIEDYQYKXILPG
- 30 NVQRIFTLNNSGSLA.IKDVLMGSAF.....SDLDGNSKNGFLKFEIDFPMQVDEGNSQWEP.....REDVMSGKT..LTLHVDVHNTSKVNSHLVGNKINLASVAG
- 31 SVTNSMSLQNSASVN.ADHIELGFSYSIDETSNPVES.....DTNPASAPGDMARMIEITAMTYDGVN.....FATSFVDANGNGWFLDELDSLPPYSSSGG.YLDN

- 1 EYDGVKPTT.DFDQVQMEIQKDDTKDE...KGLMVQNKYGNISIKLQFSFEATQWNLGTLIK.KDHTDKDGVYKENEKAHSEDKN
- 2 EKGGLAAGT...EDYLVQVFEFVD...GKDNIFQGDNTLEWTFNANQEGEEK
- 3 EKG.ISAGK...SDKFKVFEFVDN...GKDNQFQGDKLQNLWTFDAQTAGAER
- 4 DVNDALWNK...YGFQDMYLIWEDT...GQPNVYQGDVCEIIVHVALAQDSSQQLSPYGFTEVPVPLPE
- 5...GGLKPGK...MDNFWIKVFEFDN...GTDQNVYQGDVCEIIVHVALAQDSSQQLSPYGFTEVPVPLPE
- 6...GITSGE...TDYLVHVLFSFEDN...DQDNQVYQGDVCEIIVHVALAQDSSQQLSPYGFTEVPVPLPE
- 7 NVRDIALASG.ETKTFSALEMQES...AGNEFQADGLDIQDFELNQRDSQ
- 8 EADGIKAQS...SDSFTVQFEFVD...GEAQNYFQKDKLTKWTFEAKQGPVKDY
- 9 DNTVGLSVN.DNMTYQVDFKKNVDETFDQ.SRFQVQNYQDEQAEINVKFEATQMPGEEQS...NGWAN
- 10 DATTVGLASG.AQTYVNVVFEFVDETSFFPG.SRLHVQNYQDEMSNLEFVFEATQMPGEDRS...ND
- 11 EYTGLPVNL.DDEVVKIKIVFEVDITDSD.VPGEVLYNQYGDIEELNFGLEATQWGLDQI.DGDAENGTIERKNANSETPKE
- 12 TPLGINSSE...TNRRIIEFKDS...GQPNVYQGMVAVAFNFDARQVMAPKYHQDQANPNGLTNGIIG.SDRATDTSNVNVAQVAVDPAFAHQD
- 13 LFDVTFANIEEG.LDQTDQIMPVRAIAI.ATNDDGKTTVLEQATAAYQVYVQ...NKQAGGVTK
- 14 QNTGLPVNPA.DFDVEMSEIEFVEYSRDA...RGVEEQNYQGDADITFTLEARQWEGQDVS...DEEYVESNEQARNGQ
- 15 TPDGKAGAGVDDHFRMVKFPEP...NVQNDLQKGAHLTFNFDARQAG.TVMNQ...IGN...ANPATIANPITNAN
- 16 SPDGDAGS...YGRYIHSFPEP...NVAQNLQGMVAVDFKFLDARQVMGNKSHNAQPNPNTIGKQGLTDTVTPNGTGDVLPDPTDKAAEDTNPQ
- 17 IFPPILKAGDHKDWLIEGKFA...ADNHYQGSSTFNMRCSGNSPTEGFEITNGAD
- 18 LFDSTVANVVEDQTLQTTQNIQVEAFGIQ.ANDIGADDKT...APSDVMKVLVQGPSKDKTGEDTKTIVGG
- 19 EGG...ALESG.ANMSIDIEISFVNNKYPN.SLFMEQKFGESINLDLIFEATQMSGEDS
- 20 EKGGLKAGN...SDTLVQVFEFVN...DKDNQFQGDVCEIIVHVALAQDSSQQLSPYGFTEVPVPLPE
- 21 ETGLKKG...KDKLQVQFEFVDN...GEDQNFQGDVCEIIVHVALAQDSSQQLSPYGFTEVPVPLPE
- 22 EGGLEAGT...SDQMYGVFEFVDN...GEDQNFQGDVCEIIVHVALAQDSSQQLSPYGFTEVPVPLPE
- 23 LLESVTMNPRAQAVTHTKLVSVDYDKNKDRYTFYSYDTSNFGYDSEAYRLNITAKTVQATKADAVELTGNREMPENFDLAAKLSKEMCR
- 24 AGFYKPLGPD...ESFDQVQVYVNL...KDAQNYQGSSTLGTNVEGGQSDVDAEFEDGTDTGSEG
- 25 EYDGVKPTA.DYDQVMEIQKNDTAKTA...DGLSVQNKYGNISIKLQFSFEATQWNLGTLIK.KDHTDKDGVYKENEKAHSEDKN
- 26 EPDGLKAGT...SDTLVQVFEFVN...KDKQVYQGDVCEIIVHVALAQDSSQQLSPYGFTEVPVPLPE
- 27 EYDGIKPNP.DYDKMEHIEIFVNDQTKD...AGHYIQNYQGDVCEIIVHVALAQDSSQQLSPYGFTEVPVPLPE
- 28 ETVDAEGLGGESRSYVHFSVPDS...AGNIEYSDKVTLEITADLEQNETQAD
- 29 KEEGVQNTSNFLDLHLTSPVESND...EHAADYSGCKFIVDFHAEVPADELAIEVADNIDLQTDAGLLDWAALLPES
- 30 PDRGILDPQ.DSDVDFIQITFKDDQTKLG...NGEYQNYKYNASVDFYFDEATQWGHVHD...SDKNKINAEINQANTPPDVTGSGGTHSNVDVND
- 31 LLAPLQVQ...SQSLMMSLFFRPE...AGNDIQGDILTMSVSTLNDASQ

Fig. S1. Sequence alignment of *Bacillus subtilis* TasA, *Bacillus cereus* CaY1/CaY2, and close primary sequences from organisms with varying evolutionary distance generated by ClustalW, covering *Bacillales*, *Chlostridia*, *Haloferacaceae*, and *Archea*. Residues conserved in more than 90% of the sequences are colored according to the Taylor coloring scheme provided by strap (<https://www.bioinformatics.org/strap/aa/>) (1). A precise description of the alignment workflow can be found in the Material and Methods section. The conserved last alanine of the signal peptide (residue 27 in TasA) is shown in bold.

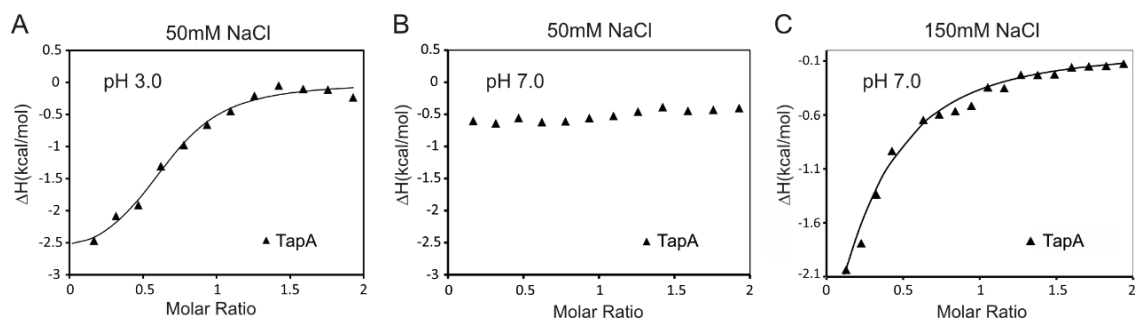


Fig. S2. ITC titration of TapA to TasA in 20 mM Tris HCl buffer with **(A)** 50 mM NaCl at pH 3.0, **(B)** 50 mM NaCl at pH 7.0 and **(C)** 150 mM NaCl at pH 7.0. At physiological pH the interaction necessitates a higher salt concentration. At acidic pH the proteins interact with lower salt but form a different, Thioflavin T stainable, fibril (as shown in [SI Appendix, Fig. S3](#)).

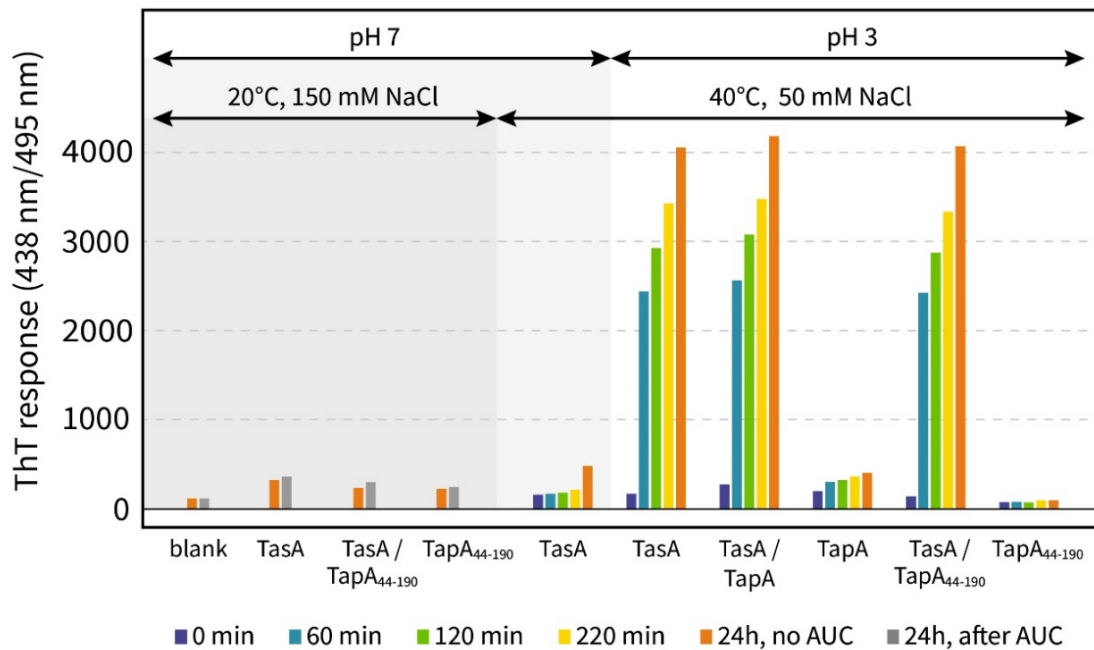


Fig. S3. Thioflavin T (ThT) assay probing stainable fiber formation upon varying multiple factors (pH, temperature, and salt concentration). For ThT response measurements, samples of 10 μ l were drawn, diluted with 90 μ l of the appropriate buffer and mixed with 100 μ l 40 μ M pH 7 buffered ThT.

At a sample condition of pH 7 at 20 $^{\circ}$ C in 20 mM phosphate buffer with 150 mM NaCl, incubation was performed with 100 μ M mature TasA₂₈₋₂₆₁, TapA₄₄₋₁₉₀ and a mixture of both (each 100 μ M) for 24 h. Under these conditions, TasA/TapA interaction was shown by ITC (SI Appendix, Fig. S2). Little to no signal is observed in the ThT assay under these conditions, indicative of no amyloid fiber species in the sample. Subsequent ultracentrifugation (as performed for filament collection) does not yield a significantly higher ThT response ensuring fiber-free samples for further experiments.

Increasing the temperature to 40 $^{\circ}$ C and decreasing the salt concentration to 50 mM in 20 mM HEPES causes a minor rise in signal for TasA (see the orange bar after 24 h) while still showing little absolute ThT response.

However, at pH 3 mature TasA₂₈₋₂₆₁ and TapA at 50 μ M (each 50 μ M when mixed) a different result is observed. Incubation at 40 $^{\circ}$ C in 20 mM HEPES and 50 mM NaCl shows a strong ThT response for TasA and TasA/TapA mixtures starting with the first datapoint measured after incubation (light blue bar, 60 min). For TapA alone, no significant response is observed. The same tendency remains when truncating the TapA C-terminus (TapA₄₄₋₁₉₀) with TapA itself showing a reduced signal.

Notably, the ThT response for mixtures of TasA and TapA is always smaller than the sum of the individual bars despite the total protein amount being doubled. This speaks toward a fold-protecting effect of TapA that prevents formation of ThT stainable, and thus likely amyloid, fibers when starting from folded protein. This effect is especially pronounced at pH 7, 20 $^{\circ}$ C and 150 mM NaCl, here shown for TapA₄₄₋₁₉₀.

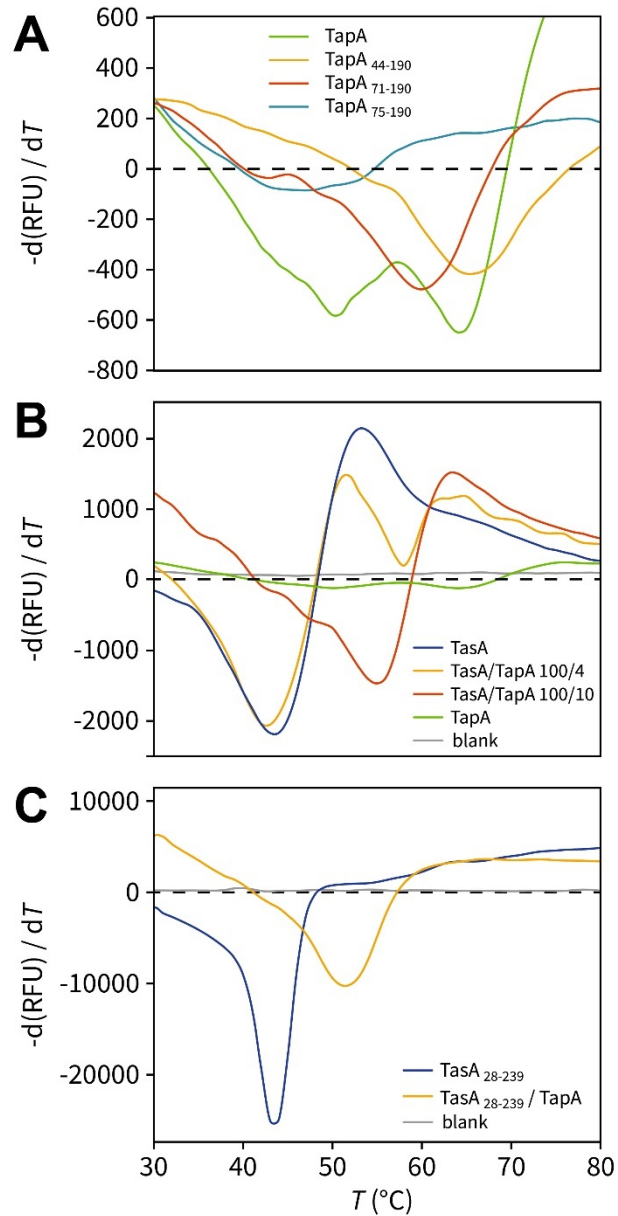


Fig. S4. Thermal shift assays (TSA) probing stability of different TapA variants and the interaction with TasA. All experiments were performed with mature TapA₄₄₋₂₅₃ and TasA₂₈₋₂₆₁ unless stated otherwise. First derivative calculations of the observed intensity show the melting curve of the individually measured samples.

(A) The highest stability is observed for TapA₄₄₋₁₉₀ with a T_m of 66 °C. In comparison, TapA₇₁₋₁₉₀ is slightly less stable with a T_m of 60 °C, pinpointing a minor contribution of N-terminal residues 44-71. A further truncation of 3 residues at the N-terminus, resulting in TapA₇₅₋₁₉₀, shows a significantly lower stability with a T_m of 46°C. Using the mature TapA, a biphasic melting profile with two peaks is observed with one at 64 °C (which likely reflects the melting of the folded domain) and one at 50 °C indicative for the C-terminus losing its association to the folded domain. Interestingly, in our X-Ray studies the most stable construct TapA₄₄₋₁₉₀ failed to crystallize in contrast to TapA₇₁₋₁₉₀ and TapA₇₅₋₁₉₀ despite the latter missing the aromatic ring packing of W74 against Y170 and P171 (Fig. 3G).

(B) TapA influences stability of TasA filaments for different mixture ratios, measured after 17 h at 20 °C. Pure TasA is shown in blue with a T_m of 43 °C. With addition of 1/10 of TapA to TasA

an T_m increase by almost 12 °C is detected (red curve). A ratio of 1/25 TapA to TasA is not sufficient to affect the TasA profile (yellow curve).

(C) C-terminally truncated TasA₂₈₋₂₃₉ (250 μM) shows a melting temperature of 44 °C. Addition of 50 μM TapA increased T_m to 53 °C showing a less pronounced effect than for the mature protein shown in **B**. A blank buffer measurement is shown in gray.

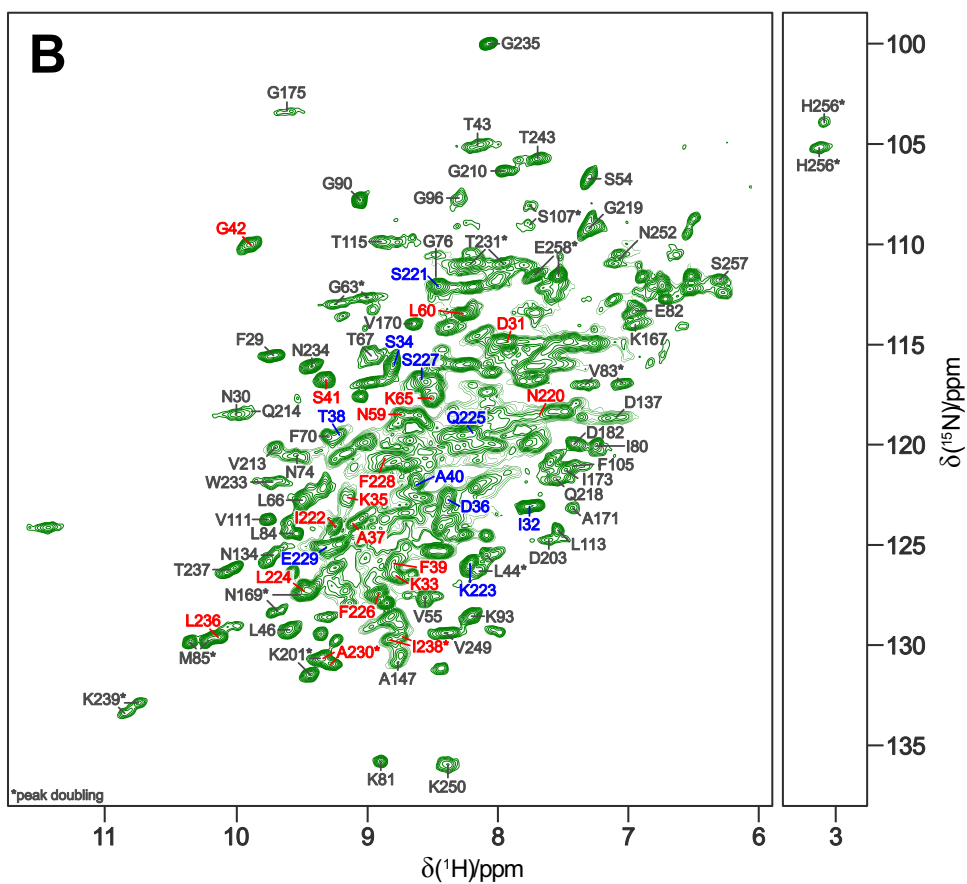
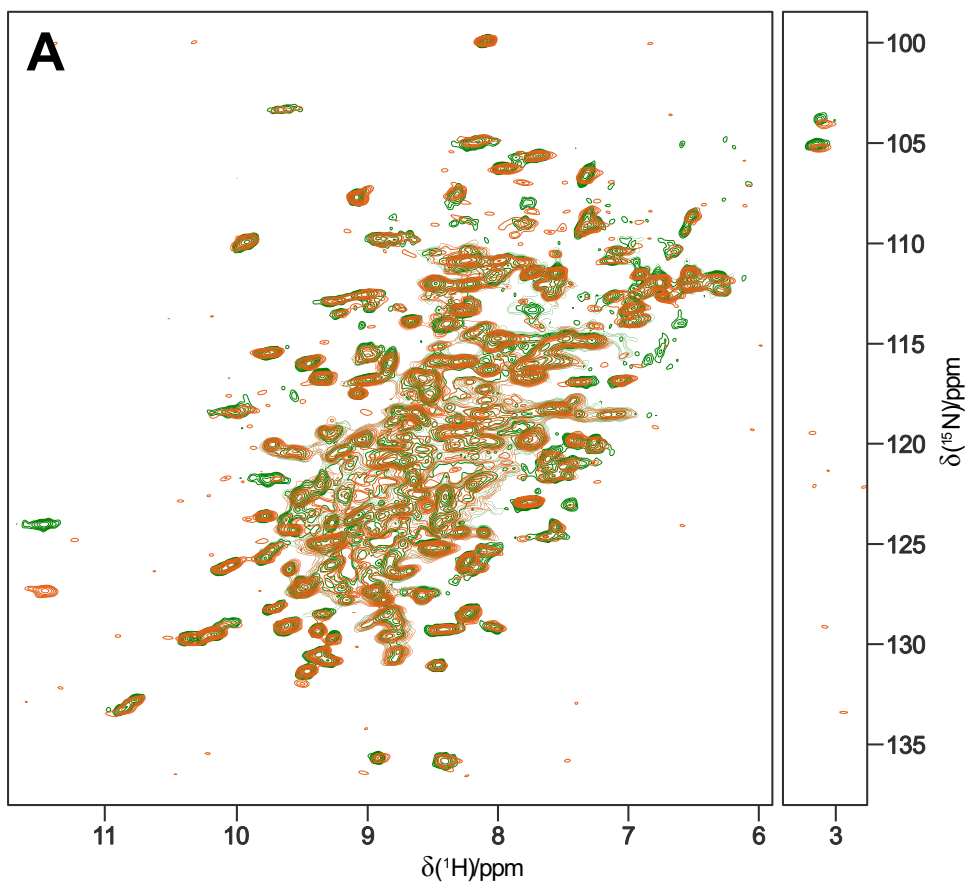


Fig. S5. (A) Comparison of ^1H - ^{15}N spectra from TapA-induced filaments of ^2H , ^{13}C , ^{15}N -labeled (100% back-exchanged) TasA (green) collected by ultracentrifugation with isotopically mixed (^2H , ^{15}N /[2- ^{13}C]; 50/50) TasA filaments generated at pH 7 through concentration (orange). The histidine sidechain signal at ~ 11.5 ppm ^1H chemical shift is aliased, its position varies due to differing spectral widths in the ^{15}N dimension. **(B)** Solid-state NMR ^1H - ^{15}N correlation of TapA-fibrillated TasA filaments as shown in **A** with assignments indicated for resolved signals. Asterisks indicate residues with peak doubling. Residues that give rise to intense signals presented in [SI Appendix, Fig. S8B](#) (antiparallel inter-strand contacts from $\beta 0$ and $\beta 9$) and [SI Appendix, Fig. S8C](#) (parallel inter-strand contacts) are indicated in red. Further signals arising from $\beta 0$ (D31-S41) and $\beta 9$ (A230-N220) are highlighted in blue. For $\beta 0$ and $\beta 9$ see also [SI Appendix, Fig. S6](#) which includes strip plots used for assignment. A complete list of assigned chemical shifts can be found in [SI Appendix, Tab. S2](#).

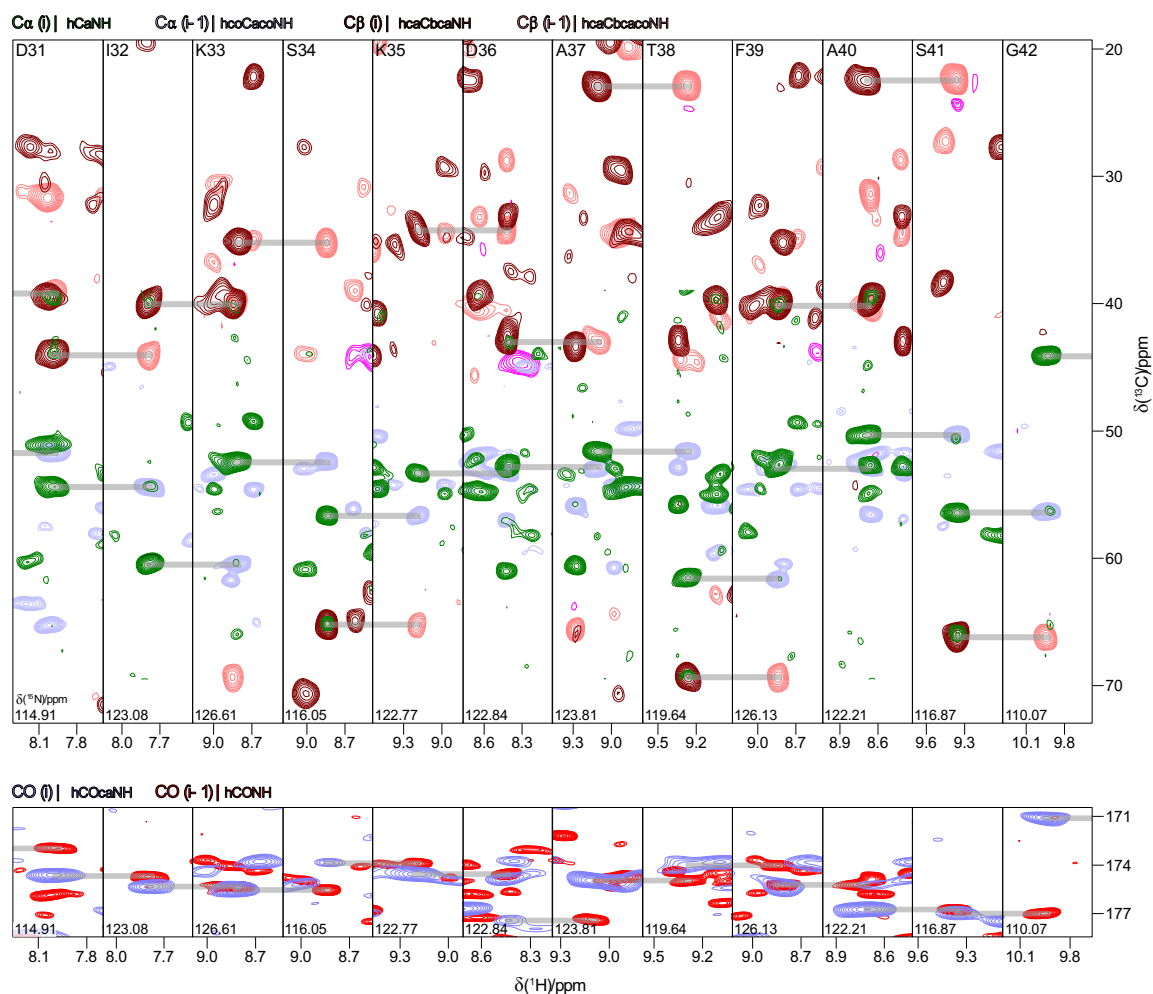


Fig. S6. Strip plots displaying NMR assignment spectra for stretches 31-42 and 220-231 (next page). Spectra are shown in green (hCaNH), light blue (hcoCAcoNH), brown (hcaCbcaNH) and light orange/pink (positive/negative contours of hcaCbcaNH) for aliphatic carbons on the top and in light blue (hCOcaNH) and red (hCONH) for carbonyls on the bottom. The spectra description above the strip plots denote whether atoms from the amino acid itself (i) or the preceding one (i-1) are measured. Connecting sequential links are highlighted with grey bars. Doubling of peaks is observed for asterisk marked residues 229, 230 and 231 (next page) whereas 231 shows clearly separated peaks in the ^1H and ^{13}C dimensions. For the other residues the effect is less pronounced and manifests as line broadening in ^1H and ^{13}C for 230 and in ^1H for 229.

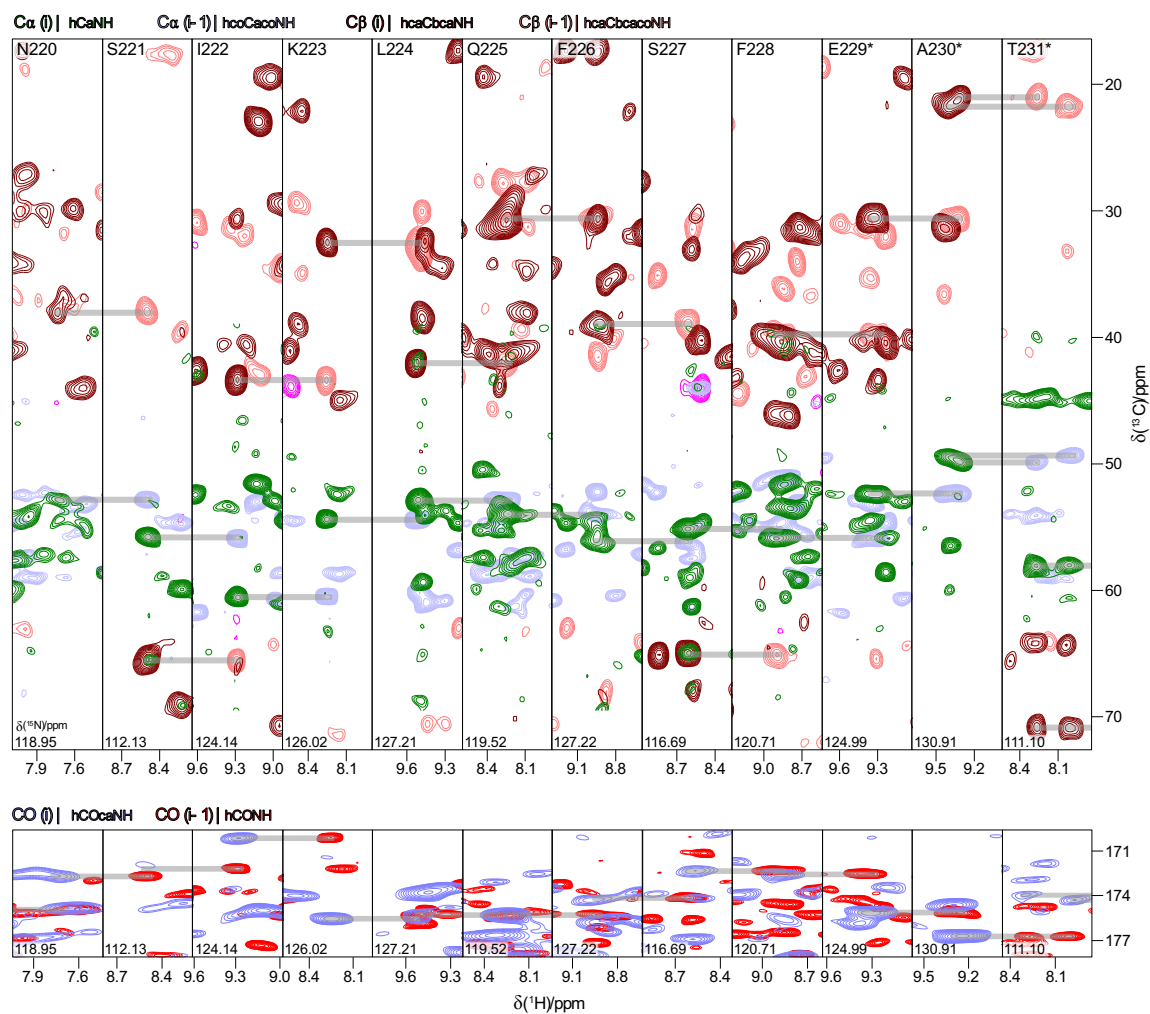


Fig. S6. continued

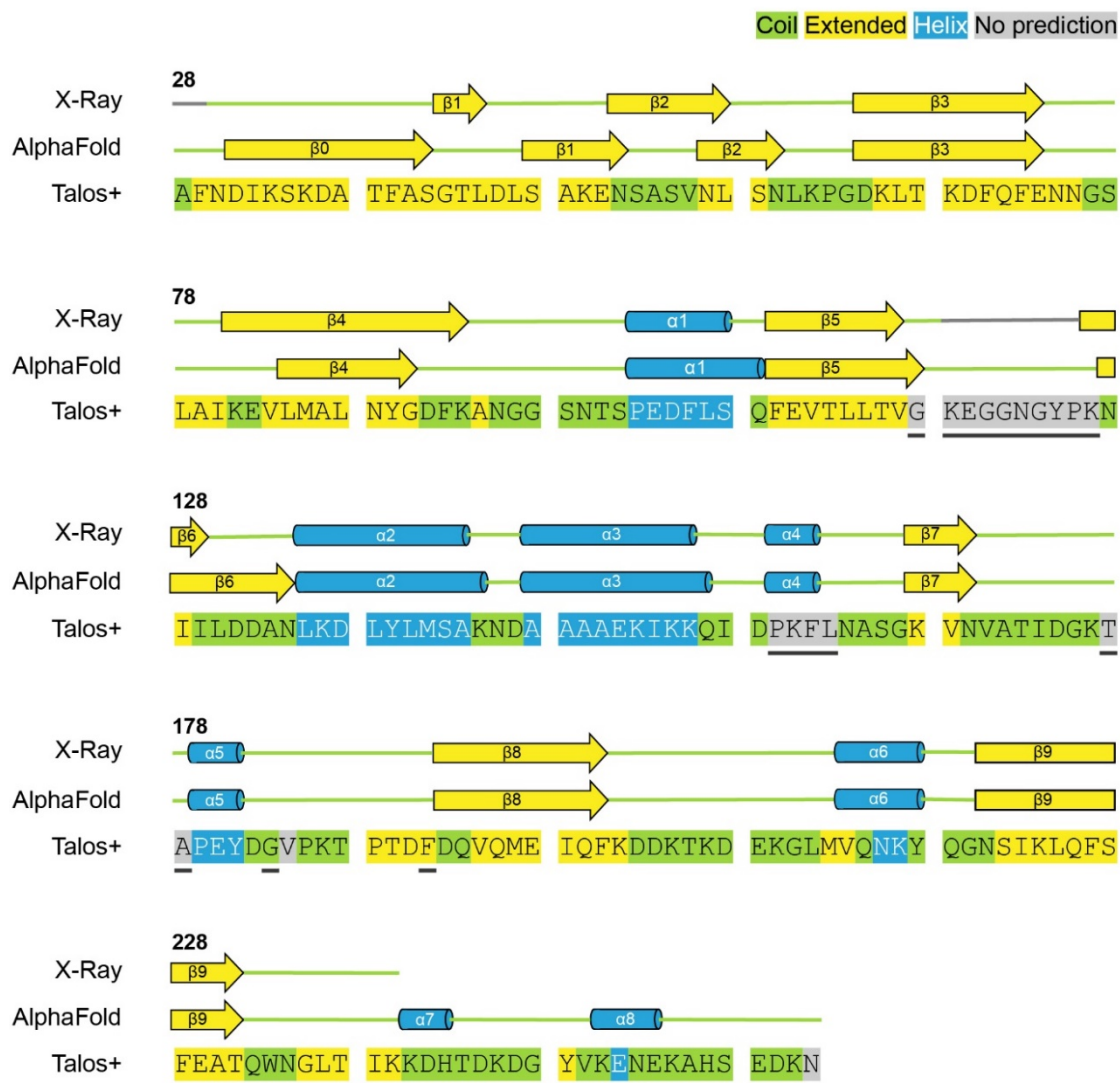


Fig. S7. Comparison of secondary structure information obtained from the X-Ray structure of monomeric TasA (PDB 5OF1), filamentous TasA predicted from AlphaFold multimer and the TALOS+ prediction based on assigned chemical shifts (SI Appendix, Tab. S2). Sheets are colored in yellow, helices in blue, coiled regions in green and not predicted (NMR) or missing regions (X-Ray) in gray. Residues lacking NMR assignments are underlined. For P185 only the C α shift is known. Fig. 3B in the main text visualized the TALOS+ prediction plotted on the X-Ray structure, SI Appendix, Fig. S11 does the same for the AlphaFold multimer model. Noteworthy is that the stretch between β_0 and β_1 is present in an extended conformation in the AlphaFold prediction and β_6 manifests as an irregular β -sheet in X-Ray and AlphaFold.

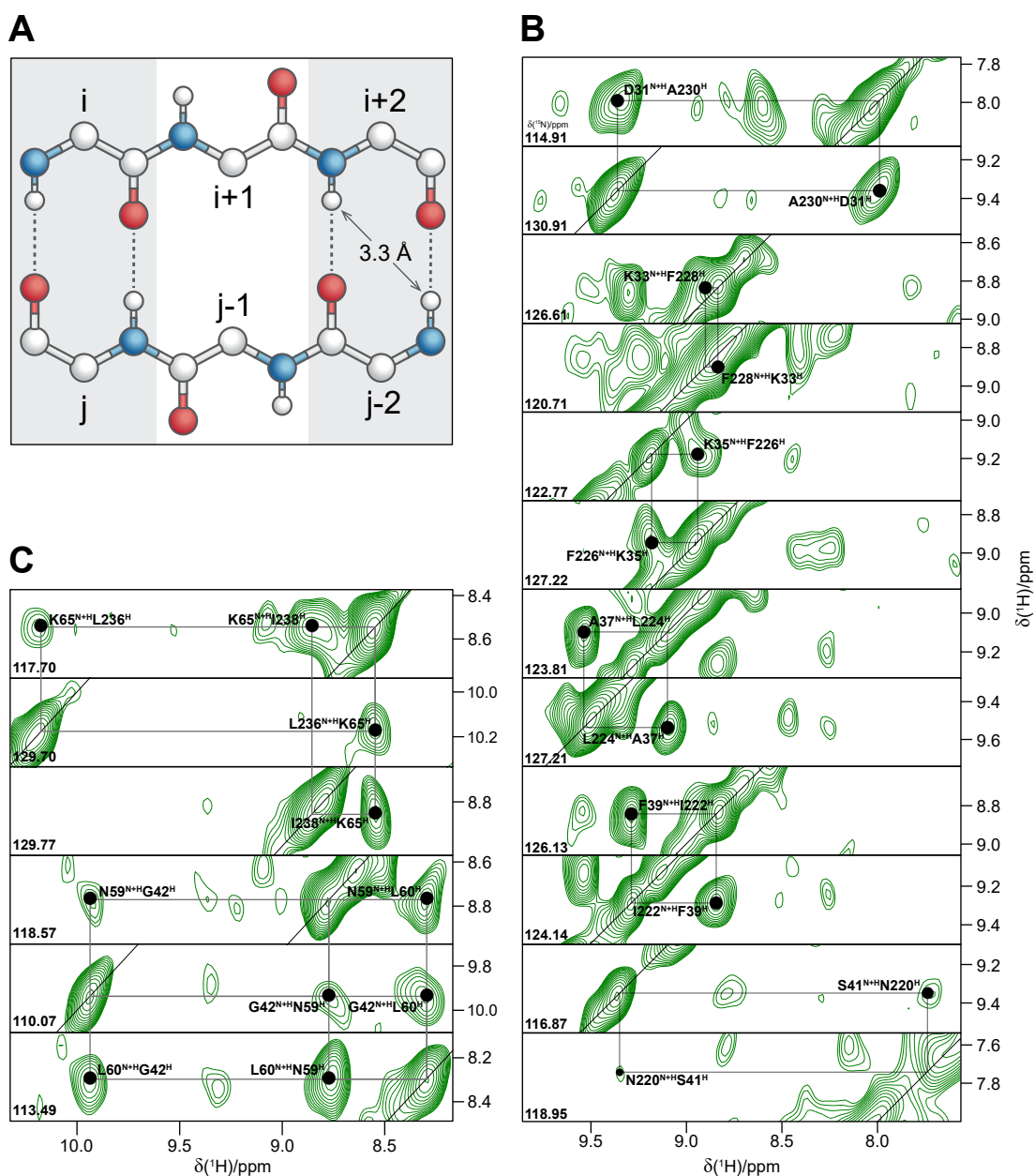


Fig. S8. NMR contacts that can be unambiguously assigned due to typical secondary structure patterns. **(A)** Schematic pattern of an antiparallel β -sheet with the cross-strand H^N-H^N distance of 3.3 Å indicated. **(B)** Slices from the solid-state NMR 3D hNHH spectrum recorded on TapA-fibrillated $^2H, ^{13}C, ^{15}N$ -labeled and 100% back-exchanged TasA filaments showing H^N-H^N contacts. Symmetric cross-peaks are characteristic for the antiparallel strands and can be attributed to β_0 and β_9 (Fig. 3D and 4C, left). **(C)** Additional slices from the spectrum shown in B. Contacts between K65 and L236/I238 (Fig. 4C, right), part of a short parallel β -sheet, are displayed on the top. On the bottom, residues G42, N59 and L60 are shown that form a less regular interaction (4C, left).

The peak doubling previously observed for A230 (SI Appendix, Figs. S5B and S6) and I238 (SI Appendix, Fig. S5B) is not resolved and appears as an increase in peak linewidth.

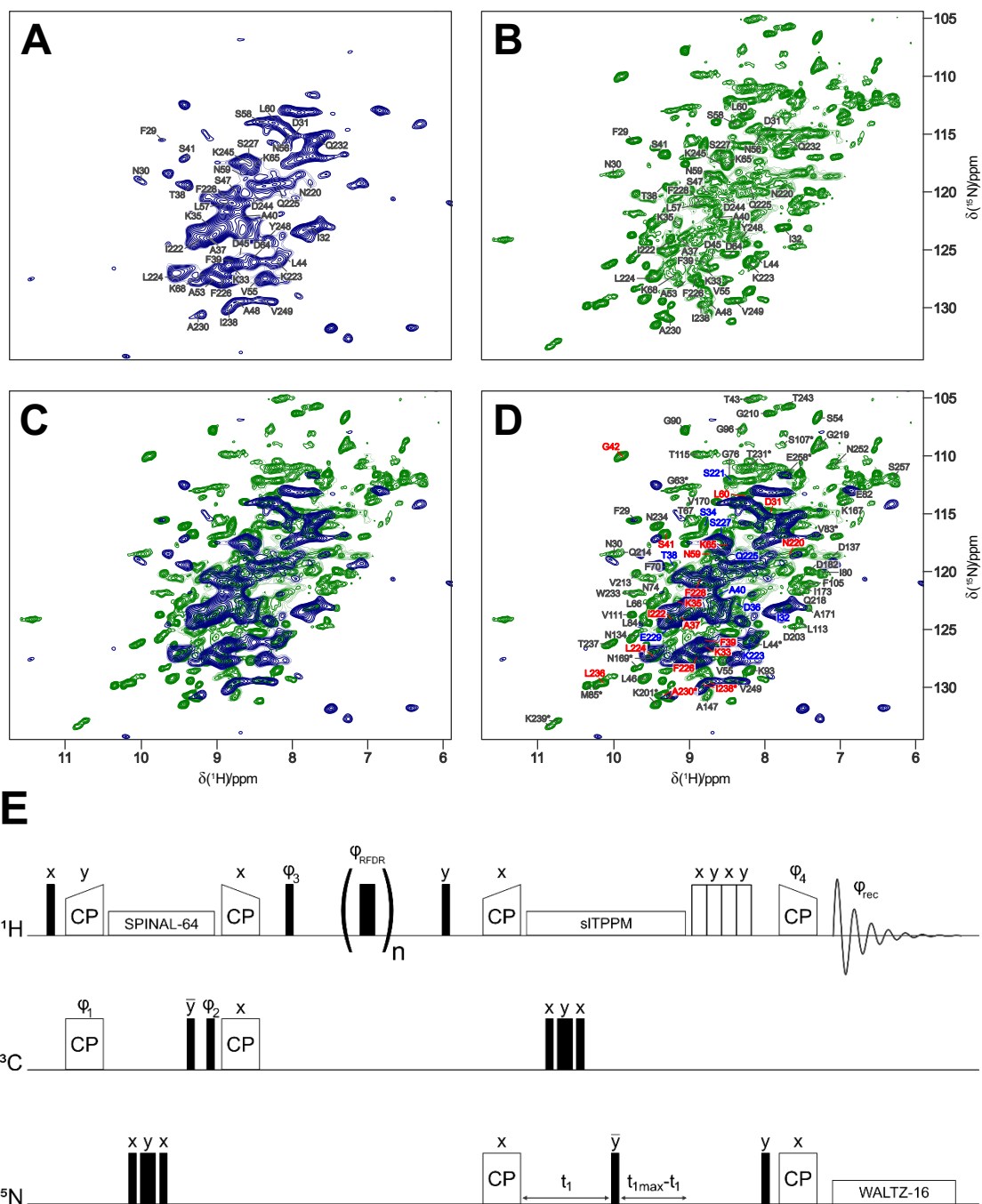


Fig. S9. Intermolecular contacts of TasA filaments monitored by NMR. **(A)** NH plane of a hchhNH experiment acquired on a sample in aqueous buffer prepared with a mixed labeling scheme (^2H , $^{15}\text{N}/[2-^{13}\text{C}]$; 50/50). Detectable peaks present at the interface are labeled. **(B)** hNH spectrum shown in [SI Appendix, Fig. S5](#) with peak labeling as presented in **A**. **(C)** Superposition of **A** and **B** without labels. **(D)** Superposition of **A** and **B** with peak labeling as presented in [SI Appendix, Fig. S5B](#). **(E)** Pulse sequence used to acquire the spectrum shown in **A**. Initial ^1H polarization is produced by a $\pi/2$ pulse. Afterwards, it is transferred to ^{13}C nuclei and back using a $^1\text{H}/^{13}\text{C}$ CP block which functions as a filter for non ^{13}C labeled material. The magnetization, now at ^1H again, is transferred through space to adjacent ^1H nuclei using an rotor-synchronized 3 ms RFDR (2) pulse train ($n=180$ at 60 kHz MAS). Subsequently a second CP block is applied, this time on $^1\text{H}/^{15}\text{N}$ filtering everything lacking ^{15}N isotopes. At the end of the pulse sequence, only magnetization that was transferred through space and experienced both ^{13}C and ^{15}N remains. For our labelling pattern this is solely true for inter-molecular cross peaks. Black rectangles depict hard pulses (narrow: $\pi/2$; broad: π), empty rectangles are used for decoupling sequences (either SPINAL-64, sITPPM or WALTZ-16), cross-polarization (CP) pulses and the

MISSISSIPPI solvent suppression scheme (xyxy pulse train prior to the last CP). Phase cycling is applied for pulses labeled with ϕ . $\phi_1=00002222$, $\phi_2=13$, $\phi_3=3311$, $\phi_4=00001111$, $\phi_{\text{RFDR}}=01011010$ (cycled within the RFDR sequence), $\phi_{\text{rec}}=20021331$.

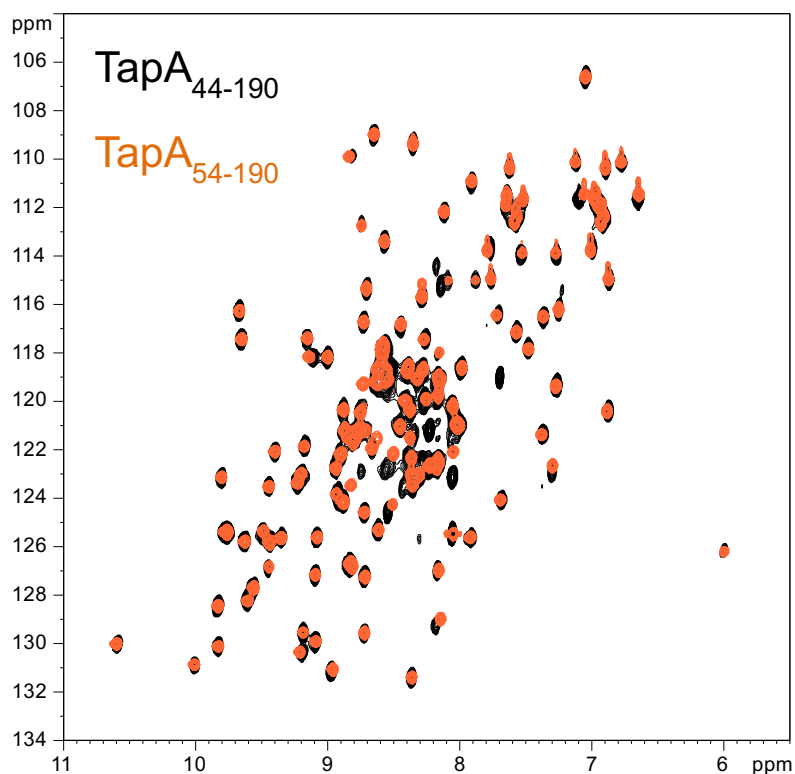
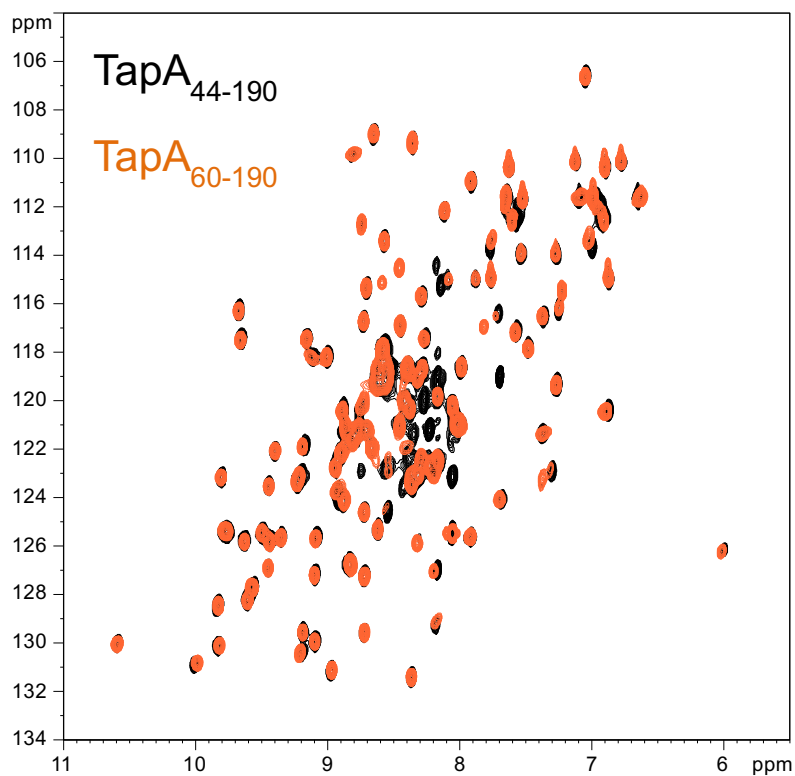


Fig. S10. Overlay of 2D solution NMR ^1H - ^{15}N correlation spectra of TapA₄₄₋₁₉₀ (black) with TapA₆₀₋₁₉₀ (orange, top) and TapA₅₄₋₁₉₀ (orange, bottom). Black signals without orange overlap are only present in spectral regions characteristic of disordered stretches and indicate an unfolded N-terminus.

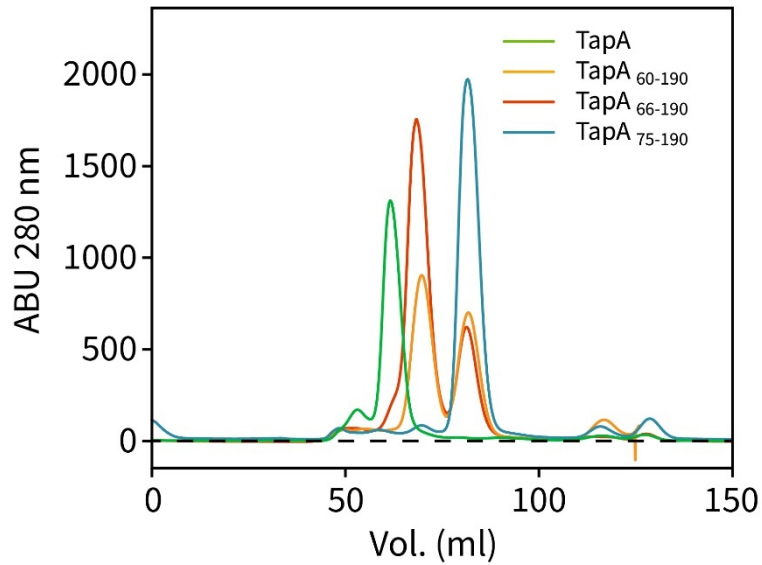


Fig. S11. TapA variants monitored by gel filtration on a Superdex 75 column (total volume 120 ml, buffer: 20 mM phosphate pH 7.0, 150 mM NaCl). Mature TapA (green curve) shows one elution maxima, characteristic of a defined monomer. For TapA variants with three cysteines like TapA₆₀₋₁₉₀ (orange curve) and TapA₆₆₋₁₉₀ (red curve) two maxima occur indicating an additional species, likely a dimer. As this effect is not present in the presence of reducing agents it can be attributed to the unbound C68 forming a disulfide bridge between two monomers. Truncating more N-terminal residues and removing C68 (TapA₇₅₋₁₉₀, blue curve) yields a monomeric profile again.

Taken together it can be concluded that C68 is likely being bound to C58 in the mature protein forming a second disulfide bridge in addition to the one observed in the crystal structure (Fig. 3E, C92-C188).

Talos+ prediction

Coil Extended Helix No prediction

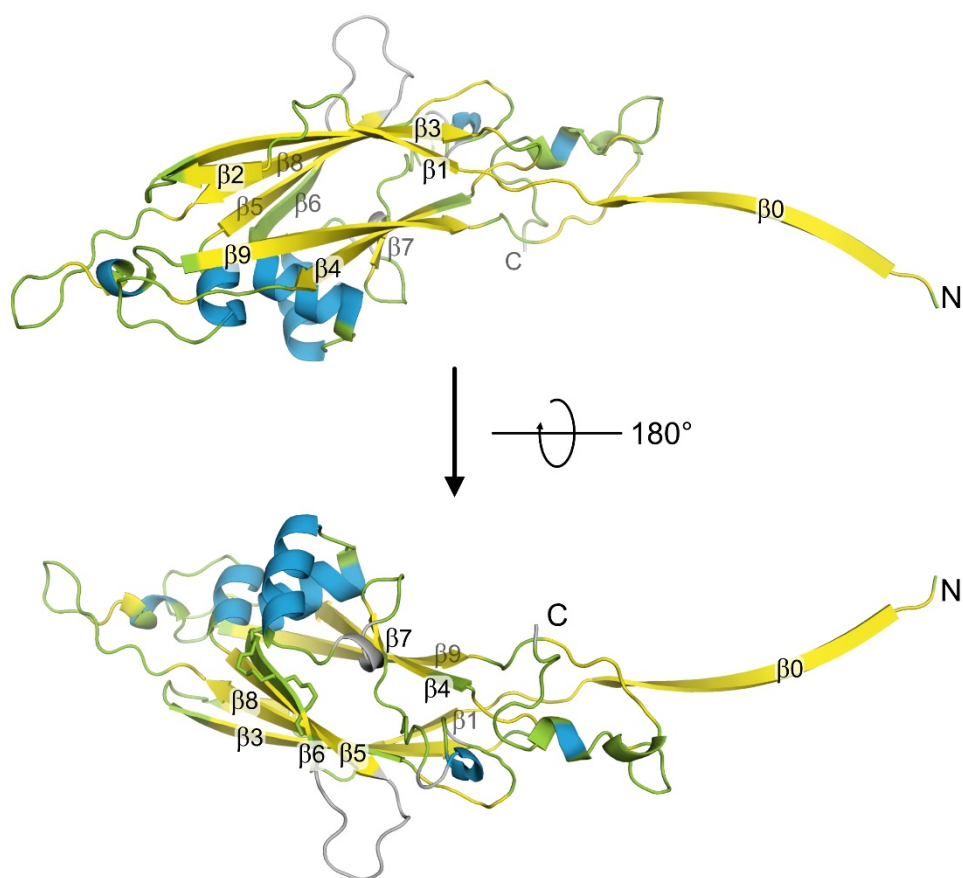


Fig. S12. TALOS+ secondary structure prediction based on solid-state NMR chemical shifts displayed on a cartoon representation of a protomer extracted from an AlphaFold multimer filament (SI Appendix, Fig. S7 and Tab. S2). Predicted helices are shown in blue, sheets in yellow, and loops in green. Regions lacking a prediction are indicated in gray. β_6 exists in an irregular conformation, similar to what is observed in the X-Ray structure (PDB 5OF1) and which is represented by the backbone trace shown on the bottom panel.

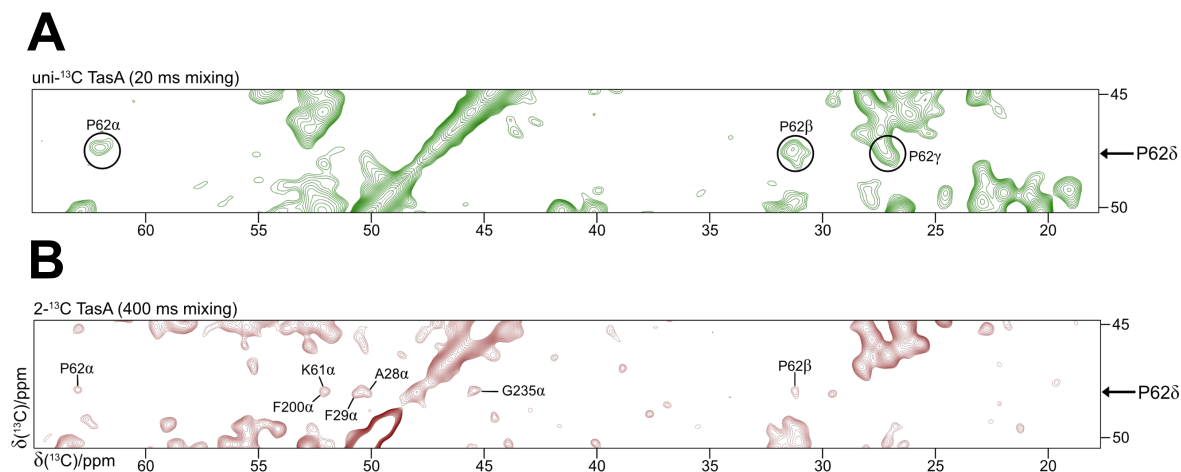


Fig. S13. ¹³C-¹³C DARR spectra showing separated peaks of P62. **(A)** Spectrum of uniformly ¹³C, ¹⁵N-labeled TasA fibers at a short mixing time of 20 ms showing intra-residue crosspeaks of P62. **(B)** Spectrum of sparsely labeled TasA fibers composed of [2-¹³C]-glycerol and uniformly ¹⁵N-labeled protein recorded with 400 ms mixing time. P62 shows crosspeaks to A28, F29, K61, F200 and G235 consistent with the predicted interface area shown in Fig. 4E. Assignment of crosspeaks was conducted by applying a correction (3) to the chemical shifts observed for the perdeuterated protein (SI Appendix, Tab. S2).

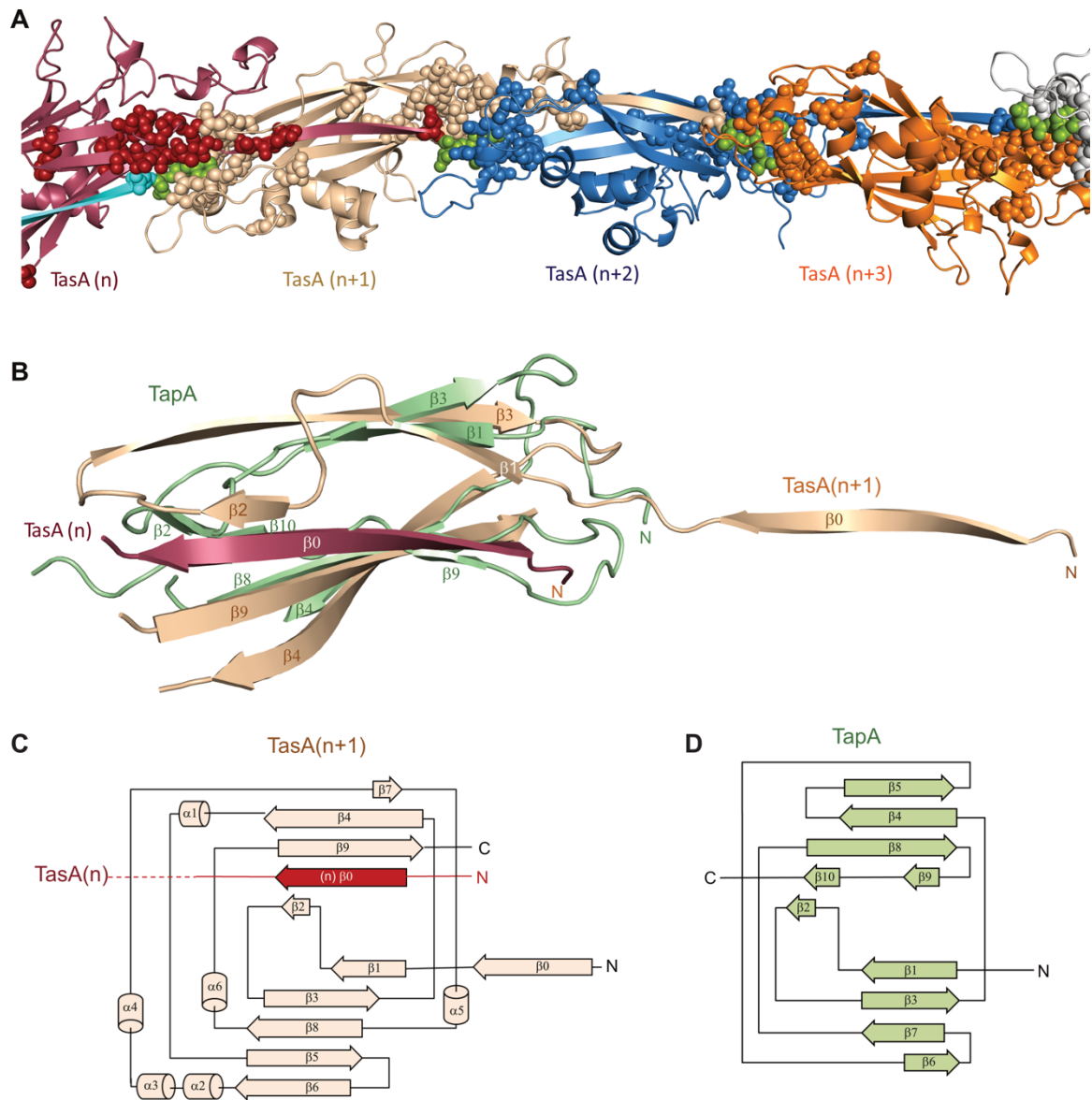


Fig. S14. (A) AlphaFold predicted TasA filament chain with the side chains of the most conserved residues indicated as spheres (see [SI Appendix, Figs. S1 and Fig. 4A](#)). All phenylalanine and alanine residues at the N-termini (A28, F29) are shown in green, other residues in the color of their protomer. (B) Overlay of TapA (green) with filamentous TasA (beige and dark red). Secondary structure topology plots of filamentous TasA (C) and TapA (D) with the same colours as in B.

Table S1. Results of AUC measurements: s-values, frictional ratios and apparent molecular weights.

Protein sample	Conc. [μM]	f/f_0	Monomer		Oligomer ^{a,b,e}	
			$S_{20,w}$	MW [kDa]	$S_{20,w}$	MW [kDa]
TapA ₄₄₋₆₂ mutant ^d	85	1.28	0.60	2.8	-	-
TapA ₇₅₋₁₉₀	100	1.24	1.69	14.9	-	-
TapA ₄₄₋₁₉₀	100	1.33	1.81	17.5	-	-
TapA ₄₄₋₂₅₃	100	1.74	1.90	27.0	-	-
TasA ₂₈₋₂₆₁	100	1.45	2.15	25.4	-	-
TasA ₂₈₋₂₆₁ ^c	100	1.35	2.97	37.2	-	-
TasA ₂₈₋₂₆₁ +TapA ₄₄₋₆₂ mutant ^d	100 + 250	1.69	2.15	32.1	9.7	~ 300
TasA ₂₈₋₂₆₁ + TapA ₇₅₋₁₉₀	100 + 100	1.37	1.93	20.5	-	-
TasA ₂₈₋₂₆₁ + TapA ₄₄₋₁₉₀	100 + 100	1.67	1.83	24.9	6.7	~ 170
TasA ₂₈₋₂₆₁ + TapA ₄₄₋₂₅₃	100 + 1	1.54	2.17	28.3	-	-
TasA ₂₈₋₂₆₁ + TapA ₄₄₋₂₅₃	100 + 2	1.58	2.18	29.4	9.8	~ 280
TasA ₂₈₋₂₆₁ + TapA ₄₄₋₂₅₃	100 + 4	1.81	2.05	33.0	9.6	~ 330
TasA ₂₈₋₂₆₁ + TapA ₄₄₋₂₅₃	100 + 10	1.95	1.94	34.3	8.8	~ 330
TasA ₂₈₋₂₆₁ + TapA ₄₄₋₂₅₃	100 + 70	1.98	1.87	32.3	6.0	~ 190
TasA ₂₈₋₂₆₁ ^c + TapA ₄₄₋₂₅₃	100 + 100	2.17	1.83	36.8	10.5	~ 500

^a Largest oligomeric species formed over the course of the sedimentation velocity experiment.

^b Potential protein fibrils could not be detected due to the high rotor speed of 40,000 rpm

^c Experiment performed with isotopic labeled ²H, ¹³C, ¹⁵N-TasA₂₈₋₂₆₁

^d TapA₄₄₋₆₂ wt: AFHDIETFDVSLQTCKDFQ; TapA₄₄₋₆₂ mutant: AFHDIETFDVSLQTSKDAQ.

^e Heterogeneous samples such as TapA-induced TasA filaments only allow to determine an approximate MW.

Table S2. Backbone assignments obtained from solid-state NMR of TasA filaments. Signal sets arising from doubled peaks are shown in italics.

Determined chemical shifts, peak lists and raw datasets have been deposited in the BMRB with the accession code 51785. Processed spectra and the CCPN 2.4.2 assignment project are uploaded to zenodo (10.5281/zenodo.7534572).

Res.	Nuc.	Shift	Res.	Nuc.	Shift	Res.	Nuc.	Shift	Res.	Nuc.	Shift
A28	C	172.04	I80	CB	38.76	<i>A143</i>	CA	52.93	E208	HN	9.01
A28	CA	50.20	I80	HN	7.22	<i>A143</i>	CB	19.49	E208	N	116.90
A28	CB	19.53	I80	N	120.18	<i>A143</i>	HN	9.00	K209	C	176.61
F29	C	176.38	K81	C	173.48	<i>A143</i>	N	124.21	K209	CA	55.27
F29	CA	50.80	K81	CA	59.09	K144	C	176.35	K209	CB	31.38
F29	CB	39.77	K81	CB	30.32	K144	CA	53.64	K209	HN	8.28
F29	HN	9.76	K81	HN	8.93	K144	CB	31.55	K209	N	119.44
F29	N	115.61	K81	N	135.94	K144	HN	6.55	G210	C	174.22
N30	C	172.98	E82	C	173.94	K144	N	112.25	G210	CA	44.35
N30	CA	51.81	E82	CA	53.36	N145	C	174.84	G210	HN	7.98
N30	CB	39.28	E82	CB	31.74	N145	CA	53.14	G210	N	106.36
N30	HN	10.04	E82	HN	6.99	N145	CB	36.99	L211	C	177.26
N30	N	118.55	E82	N	112.92	N145	HN	7.73	L211	CA	53.22
D31	C	174.68	V83	C	173.69	N145	N	119.52	L211	CB	40.80
D31	CA	54.39	V83	CA	61.63	D146	C	176.45	L211	HN	8.39
D31	CB	43.97	V83	CB	31.00	D146	CA	54.65	L211	N	123.77
D31	HN	7.98	V83	HN	7.37	D146	CB	44.06	M212	C	175.36
D31	N	114.89	V83	N	117.06	D146	HN	7.53	M212	CA	53.30
I32	C	175.36	V83	<i>C</i>	173.60	D146	N	118.43	M212	CB	33.02
I32	CA	60.48	V83	CA	61.75	A147	C	180.05	V213	C	172.79
I32	CB	39.98	V83	CB	31.01	A147	CA	54.58	V213	CA	58.58
I32	HN	7.79	V83	HN	7.07	A147	CB	17.82	V213	CB	35.12
I32	N	123.08	V83	N	116.97	A147	HN	8.79	V213	HN	9.73
K33	C	175.52	L84	C	176.59	A147	N	130.76	V213	N	120.21
K33	CA	52.43	L84	CA	52.39	A148	C	181.25	Q214	C	176.71
K33	CB	35.21	L84	CB	42.72	A148	CA	54.47	Q214	CA	57.53
K33	HN	8.81	L84	HN	9.60	A148	CB	16.77	Q214	CB	27.66
K33	N	126.61	L84	N	124.23	A148	HN	8.20	Q214	HN	9.82
S34	C	173.90	M85	C	174.37	A148	N	122.19	Q214	N	118.23
S34	CA	56.68	M85	CA	54.62	A149	C	179.60	N215	C	178.40
S34	CB	65.18	M85	CB	34.95	A149	CA	54.46	N215	CA	55.43
S34	HN	8.83	M85	HN	10.39	A149	CB	18.80	N215	CB	37.94
S34	N	116.05	M85	N	129.89	A149	HN	8.75	N215	HN	8.11
K35	C	174.57	M85	<i>C</i>	174.38	A149	N	123.42	N215	N	117.36
K35	CA	53.32	M85	CA	54.28	A150	C	179.51	K216	C	174.77
K35	CB	34.15	M85	CB	34.79	A150	CA	54.46	K216	CA	57.53
K35	HN	9.19	M85	HN	10.25	A150	CB	17.28	K216	CB	29.83
K35	N	122.78	M85	N	129.76	A150	HN	8.03	K216	HN	7.62
D36	C	177.43	A86	C	173.85	A150	N	118.26	K216	N	118.35
D36	CA	52.94	A86	CA	49.32	A150	<i>C</i>	179.49	Y217	C	176.83
D36	CB	42.77	A86	CB	22.14	A150	CA	54.30	Y217	CA	57.08
D36	HN	8.42	A86	HN	8.69	A150	CB	17.42	Y217	CB	37.55
D36	N	122.84	A86	N	126.47	A150	HN	8.12	Y217	HN	7.74
A37	C	174.98	A86	<i>C</i>	174.02	A150	N	118.07	Y217	N	116.12
A37	CA	51.59	A86	CA	49.45	E151	C	178.86	Y217	<i>C</i>	176.77
A37	CB	22.92	A86	CB	22.09	E151	CA	58.62	Y217	CA	57.37

A37	HN	9.11	A86	HN	8.45	E151	CB	28.42	Y217	CB	37.51
A37	N	123.81	A86	N	125.36	E151	HN	7.81	Y217	HN	7.55
T38	C	174.04	L87	C	173.49	E151	N	116.26	Y217	N	116.08
T38	CA	61.62	L87	CA	52.63	K152	C	179.96	Q218	C	176.66
T38	CB	69.30	L87	CB	45.57	K152	CA	58.84	Q218	CA	58.33
T38	HN	9.27	L87	HN	7.74	K152	CB	31.35	Q218	CB	27.60
T38	N	119.64	L87	N	120.02	K152	HN	7.41	Q218	HN	7.56
F39	C	175.12	N88	C	173.13	K152	N	118.18	Q218	N	121.62
F39	CA	52.89	N88	CA	50.40	I153	C	178.72	G219	C	174.94
F39	CB	40.16	N88	CB	41.58	I153	CA	62.18	G219	CA	45.19
F39	HN	8.85	N88	HN	8.35	I153	CB	35.06	G219	HN	7.32
F39	N	126.13	N88	N	120.10	I153	HN	8.09	G219	N	109.25
A40	C	176.77	Y89	C	173.63	I153	N	120.00	N220	C	172.67
A40	CA	50.32	Y89	CA	55.75	K154	C	177.99	N220	CA	52.83
A40	CB	22.45	Y89	CB	41.57	K154	CA	59.05	N220	CB	38.00
A40	HN	8.69	Y89	HN	8.27	K154	CB	31.48	N220	HN	7.74
A40	N	122.22	Y89	N	116.00	K154	HN	8.76	N220	N	118.82
S41	C	177.00	G90	C	171.28	K154	N	119.79	S221	C	172.21
S41	CA	56.42	G90	CA	44.10	K155	C	177.11	S221	CA	55.82
S41	CB	66.18	G90	HN	9.09	K155	CA	57.47	S221	CB	65.55
S41	HN	9.36	G90	N	107.82	K155	CB	31.54	S221	HN	8.49
S41	N	116.79	D91	C	174.31	K155	HN	7.29	S221	N	112.13
G42	C	171.05	D91	CA	54.69	K155	N	114.85	I222	C	170.14
G42	CA	44.11	D91	CB	40.34	Q156	C	174.62	I222	CA	60.55
G42	HN	9.93	D91	HN	8.50	Q156	CA	54.85	I222	CB	43.37
G42	N	110.07	D91	N	117.01	Q156	CB	30.20	I222	HN	9.28
T43	C	172.22	F92	C	175.54	Q156	HN	8.06	I222	N	124.14
T43	CA	58.66	F92	CA	57.69	Q156	N	115.26	K223	C	175.55
T43	CB	71.63	F92	CB	39.50	I157	CA	59.31	K223	CA	54.43
T43	HN	8.20	F92	HN	8.61	I157	CB	40.49	K223	CB	32.50
T43	N	105.17	F92	N	118.65	I157	HN	7.63	K223	HN	8.25
L44	C	173.95	K93	C	173.48	I157	N	120.81	K223	N	126.02
L44	CA	52.44	K93	CA	54.13	D158	CA	53.58	L224	C	175.38
L44	CB	45.01	K93	CB	34.72	D158	HN	9.08	L224	CA	52.90
L44	HN	8.18	K93	HN	8.23	D158	N	119.92	L224	CB	42.04
L44	N	126.30	K93	N	128.59	N163	C	176.13	L224	HN	9.52
L44	CA	52.11	A94	CA	52.50	N163	CA	51.90	L224	N	127.28
L44	CB	44.79	A94	CB	18.26	N163	CB	41.74	Q225	C	175.34
L44	HN	8.05	A94	HN	8.30	A164	C	177.97	Q225	CA	54.01
L44	N	125.49	A94	N	124.50	A164	CA	54.25	Q225	CB	30.66
D45	C	173.07	N95	C	174.99	A164	CB	17.50	Q225	HN	8.24
D45	CA	53.08	N95	HN	8.78	A164	HN	8.94	Q225	N	119.52
D45	CB	43.29	N95	N	121.42	A164	N	127.46	F226	C	174.15
D45	HN	8.80	G96	C	175.03	S165	C	174.76	F226	CA	56.14
D45	N	125.55	G96	CA	44.90	S165	CA	58.88	F226	CB	38.95
L46	C	175.36	G96	HN	8.33	S165	CB	64.11	F226	HN	8.95
L46	CA	53.06	G96	N	107.64	S165	HN	8.29	F226	N	127.22
L46	CB	44.09	G97	C	173.92	S165	N	111.43	S227	C	172.35
L46	HN	9.62	G97	CA	45.03	G166	C	171.90	S227	CA	55.16
L46	N	129.31	G97	HN	7.84	G166	CA	44.65	S227	CB	65.05
S47	C	173.55	G97	N	111.04	G166	HN	8.18	S227	HN	8.62

S47	CA	55.97	S98	C	176.37	G166	N	110.81	S227	N	116.69
S47	CB	62.39	S98	CA	59.51	K167	C	174.67	F228	C	172.57
S47	HN	8.69	S98	CB	62.75	K167	CA	55.46	F228	CA	55.91
S47	N	119.77	S98	HN	8.48	K167	CB	36.03	F228	CB	39.81
S47	CA	56.04	S98	N	115.89	K167	HN	6.99	F228	HN	8.90
S47	CB	62.96	N99	C	173.88	K167	N	113.61	F228	N	120.71
S47	HN	8.84	N99	CA	54.83	V168	C	175.87	E229	C	175.11
S47	N	119.12	N99	CB	39.66	V168	CA	60.13	E229	CA	52.42
A48	C	174.75	N99	HN	9.05	V168	CB	33.75	E229	CB	30.64
A48	CA	49.77	N99	N	119.89	V168	HN	7.72	E229	HN	9.33
A48	CB	20.08	T100	C	174.41	V168	N	116.74	E229	N	124.99
A48	HN	8.80	T100	CA	60.02	N169	C	173.92	A230	C	176.76
A48	N	130.00	T100	CB	69.03	N169	CA	52.70	A230	CA	49.87
A48	C	174.75	T100	HN	8.23	N169	CB	38.01	A230	CB	21.11
A48	CA	49.89	T100	N	112.14	N169	HN	9.49	A230	HN	9.33
A48	CB	19.87	S101	CA	52.99	N169	N	127.30	A230	N	130.91
A48	HN	8.77	S101	CB	62.80	N169	C	174.16	A230	C	176.74
A48	N	128.93	S101	HN	7.45	N169	CA	53.24	A230	CA	49.42
K49	C	174.76	S101	N	115.01	N169	CB	38.45	A230	CB	21.67
K49	CA	54.40	P102	C	178.59	N169	HN	9.73	A230	HN	9.40
K49	CB	34.44	P102	CA	63.64	N169	N	128.33	A230	N	130.81
K49	HN	8.86	P102	CB	31.37	V170	C	173.82	T231	C	174.31
K49	N	123.69	E103	C	178.41	V170	CA	58.57	T231	CA	58.00
K49	C	174.62	E103	CA	60.22	V170	CB	30.22	T231	CB	70.90
K49	CA	54.41	E103	CB	27.67	V170	HN	8.68	T231	HN	8.00
K49	CB	34.80	E103	HN	8.17	V170	N	114.01	T231	N	111.10
K49	HN	8.71	E103	N	114.51	A171	C	176.73	T231	C	173.98
K49	N	123.49	D104	C	179.95	A171	CA	49.40	T231	CA	58.00
E50	C	175.20	D104	CA	57.02	A171	CB	17.63	T231	CB	70.83
E50	CA	54.74	D104	CB	38.00	A171	HN	7.45	T231	HN	8.27
E50	CB	29.51	D104	HN	8.08	A171	N	123.09	T231	N	110.99
E50	HN	8.94	D104	N	119.89	T172	C	174.83	Q232	C	177.11
E50	N	123.63	F105	C	177.34	T172	CA	61.36	Q232	CA	53.52
N51	C	174.31	F105	CA	58.90	T172	HN	9.03	Q232	CB	32.17
N51	CA	51.80	F105	CB	37.76	T172	N	121.05	Q232	HN	7.69
N51	CB	38.78	F105	HN	7.48	I173	C	175.81	Q232	N	115.50
N51	HN	8.48	F105	N	121.13	I173	CA	58.28	Q232	C	177.15
N51	N	125.46	L106	C	177.63	I173	CB	34.36	Q232	CA	53.53
S52	C	173.18	L106	CA	57.45	I173	HN	7.50	Q232	CB	31.93
S52	CA	56.95	L106	CB	40.83	I173	N	121.34	Q232	HN	7.50
S52	CB	62.79	L106	HN	8.37	D174	C	177.20	Q232	N	114.88
S52	HN	7.32	L106	N	118.31	D174	CA	55.05	W233	C	173.89
S52	N	114.88	L106	CA	57.41	D174	CB	40.67	W233	CA	57.54
A53	C	177.90	L106	CB	40.85	D174	HN	9.28	W233	CB	27.19
A53	CA	54.67	L106	HN	8.42	D174	N	129.82	W233	HN	9.75
A53	CB	17.29	L106	N	119.43	G175	C	173.36	W233	N	121.95
A53	HN	9.19	S107	C	175.12	G175	CA	45.19	N234	C	173.29
A53	N	127.60	S107	CA	58.98	G175	HN	9.61	N234	CA	52.38
S54	C	173.76	S107	CB	63.11	G175	N	103.43	N234	CB	38.22
S54	CA	57.07	S107	HN	7.82	K176	C	177.11	N234	HN	9.45
S54	CB	64.28	S107	N	109.02	K176	CA	59.68	N234	N	116.10

S54	HN	7.34	S107	CA	58.84	K176	CB	33.18	G235	C	172.42
S54	N	106.73	S107	CB	63.07	K176	HN	7.80	G235	CA	45.24
V55	C	175.85	S107	HN	7.77	K176	N	120.02	G235	HN	8.10
V55	CA	65.26	S107	N	108.15	P179	C	178.57	G235	N	100.02
V55	CB	31.70	Q108	C	172.55	P179	CA	64.35	L236	C	175.59
V55	HN	8.59	Q108	CA	54.03	P179	CB	31.12	L236	CA	52.47
V55	N	127.68	Q108	CB	27.06	E180	C	177.52	L236	CB	45.29
N56	C	174.58	Q108	HN	8.00	E180	CA	57.82	L236	HN	10.18
N56	CA	51.12	Q108	N	118.86	E180	CB	30.12	L236	N	129.72
N56	CB	39.41	Q108	CA	54.19	E180	HN	8.66	T237	C	174.52
N56	HN	8.02	Q108	CB	27.14	E180	N	118.52	T237	CA	63.05
N56	N	114.86	Q108	HN	8.08	E180	CA	57.93	T237	CB	66.09
L57	C	175.64	Q108	N	119.29	E180	CB	30.54	T237	HN	10.08
L57	CA	53.36	F109	C	174.99	E180	HN	8.79	T237	N	126.29
L57	CB	46.20	F109	CA	55.90	E180	N	118.98	I238	C	176.94
L57	HN	8.93	F109	CB	41.24	Y181	C	174.52	I238	CA	61.51
L57	N	121.14	F109	HN	7.68	Y181	CA	58.75	I238	CB	36.43
L57	CA	53.54	F109	N	116.06	Y181	CB	38.85	I238	HN	8.86
L57	CB	46.21	E110	C	174.75	Y181	HN	8.08	I238	N	129.69
L57	HN	8.81	E110	CA	53.30	Y181	N	116.49	I238	C	176.94
L57	N	120.76	E110	CB	32.31	D182	CA	53.76	I238	CA	61.56
S58	C	174.53	E110	HN	9.08	D182	CB	42.31	I238	CB	36.27
S58	CA	55.39	E110	N	117.64	D182	HN	7.45	I238	HN	8.78
S58	CB	64.06	V111	C	175.62	D182	N	119.94	I238	N	129.68
S58	HN	8.41	V111	CA	61.23	V184	CA	64.95	K239	C	177.95
S58	N	114.23	V111	CB	31.53	V184	CB	30.04	K239	CA	52.99
N59	C	174.31	V111	HN	9.79	V184	HN	8.52	K239	CB	33.99
N59	CA	53.07	V111	N	123.74	V184	N	117.06	K239	HN	10.85
N59	CB	39.49	T112	C	175.84	P185	CA	63.18	K239	N	133.26
N59	HN	8.77	T112	CA	61.39	K186	CA	56.18	K240	C	178.29
N59	N	118.47	T112	CB	67.96	K186	CB	31.30	K240	CA	59.16
L60	C	176.60	T112	HN	8.58	K186	HN	7.85	K240	CB	31.32
L60	CA	55.00	T112	N	116.83	K186	N	118.17	K240	HN	8.73
L60	CB	44.52	L113	C	174.01	T187	CA	58.91	K240	N	121.05
L60	HN	8.29	L113	CA	55.80	T187	CB	71.51	D241	C	176.80
L60	N	113.49	L113	CB	44.27	T187	HN	7.59	D241	CA	55.10
K61	C	171.72	L113	HN	7.58	T187	N	115.01	D241	CB	39.48
K61	CA	52.16	L113	N	124.23	P188	C	172.83	D241	HN	8.24
K61	CB	33.96	L114	C	174.94	P188	CA	58.68	D241	N	113.03
K61	HN	9.19	L114	CA	53.49	P188	CB	34.79	H242	C	175.70
K61	N	120.42	L114	CB	44.04	T189	C	173.04	H242	CA	55.77
P62	C	175.83	L114	HN	7.61	T189	CA	61.15	H242	CB	33.46
P62	CA	63.17	L114	N	118.40	T189	CB	70.73	H242	HN	7.84
P62	CB	30.58	T115	CA	58.50	T189	HN	8.96	H242	N	116.81
G63	C	175.02	T115	CB	70.96	T189	N	124.47	T243	C	175.28
G63	CA	44.03	T115	HN	8.91	D190	CA	53.00	T243	CA	58.61
G63	HN	9.27	T115	N	109.96	D190	CB	45.72	T243	CB	71.88
G63	N	113.03	V116	CA	61.22	D190	HN	9.39	T243	HN	7.73
G63	C	175.07	V116	CB	34.21	D190	N	129.44	T243	N	105.78
G63	CA	44.06	V116	HN	8.34	D192	C	177.97	D244	C	179.25
G63	HN	9.03	V116	N	119.55	D192	CA	54.48	D244	CA	51.88

G63	N	112.70	N127	C	173.64	D192	CB	40.26	D244	CB	41.33
D64	C	175.23	N127	CA	52.16	Q193	C	174.61	D244	HN	8.58
D64	CA	55.70	N127	CB	38.73	Q193	CA	56.91	D244	N	120.38
D64	CB	41.16	I128	C	175.64	Q193	CB	28.76	K245	CA	58.36
D64	HN	8.53	I128	CA	61.64	Q193	HN	8.62	K245	CB	30.59
D64	N	125.28	I128	CB	36.33	Q193	N	123.77	K245	HN	8.55
K65	C	174.15	I128	HN	8.74	V194	C	174.94	K245	N	117.27
K65	CA	54.52	I128	N	125.02	V194	CA	61.08	G247	C	173.01
K65	CB	35.75	I129	C	175.50	V194	CB	33.19	G247	CA	45.11
K65	HN	8.53	I129	CA	63.14	V194	HN	8.43	G247	HN	8.26
K65	N	117.69	I129	CB	37.82	V194	N	122.79	G247	N	111.13
L66	C	174.95	I129	HN	8.82	Q195	C	174.01	Y248	C	178.00
L66	CA	52.91	I129	N	129.01	Q195	CA	54.27	Y248	CA	58.09
L66	CB	44.02	L130	C	179.25	Q195	CB	32.42	Y248	CB	37.88
L66	HN	9.54	L130	CA	52.80	Q195	HN	9.46	Y248	HN	8.25
L66	N	122.79	L130	CB	41.15	Q195	N	127.37	Y248	N	123.23
T67	C	175.18	L130	HN	7.64	M196	C	174.46	V249	C	176.07
T67	CA	60.83	L130	N	115.41	M196	CA	53.29	V249	CA	61.55
T67	CB	70.60	D131	C	173.03	M196	CB	35.29	V249	CB	27.79
T67	HN	9.00	D131	CA	53.18	M196	HN	9.37	V249	HN	8.42
T67	N	115.62	D131	CB	43.80	M196	N	122.21	V249	N	129.44
K68	C	173.49	D131	HN	8.31	E197	C	175.89	K250	C	179.75
K68	CA	53.76	D131	N	119.49	E197	CA	54.44	K250	CA	56.91
K68	CB	34.22	D132	C	175.50	E197	CB	30.07	K250	CB	30.98
K68	HN	9.44	D132	CA	55.59	E197	HN	9.35	K250	HN	8.42
K68	N	127.23	D132	CB	39.98	E197	N	125.30	K250	N	135.93
K68	CA	53.60	D132	HN	7.50	I198	C	173.60	E251	C	177.60
K68	CB	34.48	D132	N	118.38	I198	CA	59.39	E251	CA	57.97
K68	HN	9.30	A133	C	176.23	I198	CB	38.98	E251	CB	28.92
K68	N	126.95	A133	CA	49.73	I198	HN	9.47	E251	HN	8.20
D69	C	174.44	A133	CB	18.69	I198	N	127.35	E251	N	120.00
D69	CA	52.77	A133	HN	8.12	Q199	C	174.56	N252	C	178.86
D69	CB	44.40	A133	N	124.59	Q199	CA	52.71	N252	CA	52.50
D69	HN	8.12	N134	C	177.15	Q199	CB	31.79	N252	CB	37.29
D69	N	121.83	N134	CA	55.07	Q199	HN	9.28	N252	HN	7.12
F70	C	173.62	N134	CB	41.20	Q199	N	126.16	N252	N	110.75
F70	CA	55.80	N134	HN	9.74	F200	C	175.22	K254	C	175.19
F70	CB	43.00	N134	N	125.45	F200	CA	52.45	K254	CA	54.75
F70	HN	9.34	L135	C	178.53	F200	CB	36.44	K254	CB	34.15
F70	N	119.58	L135	CA	58.05	F200	HN	8.86	A255	C	176.03
Q71	C	174.08	L135	CB	40.23	F200	N	128.57	A255	CA	51.23
Q71	CA	53.14	L135	HN	9.05	K201	C	174.76	A255	CB	18.06
Q71	CB	31.53	L135	N	125.77	K201	CA	56.65	A255	HN	8.04
Q71	HN	8.64	K136	C	178.07	K201	CB	31.38	A255	N	120.23
Q71	N	120.19	K136	CA	59.63	K201	HN	9.46	A255	C	177.22
F72	C	175.01	K136	CB	28.84	K201	N	131.47	A255	CA	51.21
F72	CA	55.87	K136	HN	8.15	K201	C	174.64	A255	CB	19.79
F72	CB	41.16	K136	N	118.68	K201	CA	56.48	H256	C	172.52
E73	C	173.66	D137	C	177.97	K201	CB	31.56	H256	CA	58.62
E73	CA	53.54	D137	CA	57.40	K201	HN	9.38	H256	CB	23.98
E73	CB	33.40	D137	CB	39.43	K201	N	130.64	H256	HN	3.18

E73	HN	9.03	D137	HN	7.15	D202	C	175.20	H256	N	105.23
E73	N	119.85	D137	N	118.68	D202	CA	52.61	H256	C	173.22
N74	C	175.00	L138	C	180.06	D202	CB	39.75	H256	CA	57.76
N74	CA	52.72	L138	CA	57.68	D202	HN	8.66	H256	CB	25.04
N74	CB	38.77	L138	CB	41.02	D202	N	121.88	H256	HN	3.14
N74	HN	9.54	L138	HN	8.12	D203	C	177.18	H256	N	104.07
N74	N	120.61	L138	N	119.37	D203	CA	52.24	S257	C	171.17
N75	C	175.42	Y139	C	175.41	D203	CB	41.15	S257	CA	54.13
N75	CA	51.83	Y139	CA	59.37	D203	HN	7.65	S257	CB	59.77
N75	CB	39.69	Y139	CB	36.81	D203	N	124.75	S257	HN	6.33
N75	HN	8.80	Y139	HN	8.43	K204	C	175.86	S257	N	111.94
N75	N	125.69	Y139	N	123.97	K204	CA	55.51	E258	C	175.79
G76	C	172.14	L140	C	180.27	K204	CB	30.63	E258	CA	51.89
G76	CA	44.03	L140	CA	57.40	K204	HN	8.95	E258	CB	33.25
G76	HN	8.52	L140	CB	40.08	K204	N	127.46	E258	HN	7.58
G76	N	110.59	L140	HN	8.65	T205	C	174.68	E258	N	111.57
S77	C	173.11	L140	N	120.90	T205	CA	65.02	E258	C	175.72
S77	CA	58.88	M141	C	176.89	T205	CB	67.90	E258	CA	52.09
S77	CB	64.16	M141	CA	59.08	T205	HN	8.21	E258	CB	33.40
S77	HN	8.47	M141	CB	33.03	T205	N	117.12	E258	HN	7.75
S77	N	115.32	M141	HN	8.59	K206	C	176.47	E258	N	111.56
L78	C	175.67	M141	N	117.05	K206	CA	54.51	D259	C	174.69
L78	CA	51.72	S142	C	175.42	K206	CB	36.23	D259	CA	54.85
L78	CB	43.34	S142	CA	60.71	K206	HN	8.88	D259	CB	39.41
L78	HN	7.91	S142	CB	64.45	K206	N	127.91	D259	HN	8.64
L78	N	121.42	S142	HN	8.04	D207	C	178.41	D259	N	122.72
A79	C	173.79	S142	N	111.75	D207	CA	51.64	K260	CA	59.95
A79	CA	52.99	A143	C	179.69	D207	CB	40.64	K260	CB	33.87
A79	CB	18.37	A143	CA	52.96	D207	HN	8.85	K260	HN	8.12
A79	HN	8.41	A143	CB	19.54	D207	N	121.00	K260	N	118.66
A79	N	122.49	A143	HN	9.08	E208	C	177.49			
I80	C	176.84	A143	N	124.93	E208	CA	58.24			
I80	CA	59.44	A143	C	179.70	E208	CB	27.78			

Table S3. X-Ray diffraction data collection and refinement statistics.

	TapA ₇₁₋₁₉₀	TapA ₇₅₋₁₉₀
Data collection		
Space group	P2 ₁ 2 ₁ 2 ₁	P2 ₁
Cell dimensions		
<i>a</i> , <i>b</i> , <i>c</i> (Å)	39.2, 52.9, 167.7	30.1, 61.1, 34.3
α , β , γ (°)	90.0, 90.0, 90.0	90.0, 106.9, 90.0
Resolution (Å)*	44.77-1.07 (1.13-1.07)	32.8-1.28 (1.36-1.28)
<i>R</i> _{meas} *	6.6 (154.2)	4.5 (177.0)
$\langle I / \sigma(I) \rangle$ *	9.77 (0.8)	14.2 (0.8)
Completeness (%)*	98.8 (97.9)	98.4 (97.2)
Multiplicity*	3.5	4.4
Refinement		
No. reflections	151,026	30,250
<i>R</i> _{work} / <i>R</i> _{free}	0.148/0.176	0.147/0.197
No. atoms		
Protein	2949	943
Ligand/ion	28	15
Water	742	212
Mean B factor (Å ²)	17.8	28.0
R.m.s deviations		
Bond lengths (Å)	0.012	0.012
Bond angles (°)	1.632	1.685
Ramachandran		
Outlier (%)	0	0
Favored (%)	96.6	95.6

* Data in highest resolution shell are indicated in parenthesis.

Table S4. H^N-H^N contacts observed by NMR within TasA filaments including those shown in [SI Appendix, Fig. S8](#). Contacts shown in column 1 are located in antiparallel β -sheets and are involved in cross-strand hydrogen bonds, the remaining show validated contacts in loop and helical regions.

D31 - A230	K65 - L236	N145 - D146	G219 - N220
K33 - F228	K65 - I138	A147 - A148	H242 - T243
K35 - F226	G42 - N59	A148 - A149	K250 - E251
A37 - L224	G42 - L60	A149 - A150	E251 - N252
F39 - I222	N59 - L60	A150 - E151	
S41 - N220	E103 - D104	E151 - K152	
S58 - V249	D104 - F105	K152 - I153	
K49 - Q71	F105 - L106	I153 - K154	
G63 - F200	S107 - Q108	K154 - K155	
K68 - M196	Q108 - F109	K155 - Q156	
F70 - V194	Y139 - L140	Q156 - I157	
M85 - V168	L140 - M141	E180 - Y181	
L84 - E229	M141 - S142	Y181 - D182	
G90 - K223	S142 - A143	N215 - K216	
K93 - S221	A143 - K144	K216 - Y217	
V111 - A133	K144 - N145	Y217 - Q218	

Table S5. Primer used for cloning different TapA fragments into pCA528.

TapA₄₄₋₂₅₃	BsmI XhoI TapA₄₄₋₂₅₃
Forward 1	5'CCAGTG CGTCTC AGGTGGT GCTTTTCATGATATTGAAAC
Reverse 1	5'TCGA CTCGAG tta CTGATCAGCTTCATTGC
<hr/>	
TapA_{44-190/33-190}	mutation for stop codon generation at AA 191
Forward 2	5'CAAATGCGATGAAT AACCGACAGTCCCTAAAAAAG
Reverse 2	5'AGGGACTGTCGGTT ATTCATCGCATTGCAAGCCTC
<hr/>	
TapA₅₄₋₁₉₀	TapA_{54ff} C-terminus Sumo
Forward 3	5'TCACTTCAAACGTGTA AAGACTTTCAGCATAACG
Reverse 3	5'TACACGTTTGA AGTGA ACCACCAATCTGTTCTCTGTGAGCCTC
<hr/>	
TapA₆₀₋₁₉₀	TapA_{60ff} C-terminus Sumo
Forward 4	5'GACTTTCAGCATACAGATA AAAACTGCCATTATG
Reverse 4	5'TCTGTATGCTG AAAGTCA CCACCAATCTGTTCTCTGTGAGCCTC
<hr/>	
TapA₆₆₋₁₉₀	TapA_{66ff} C-terminus Sumo
Forward 5	5'AAAACTGCCATTATGATA AAACGCTGGGATCAAAG
Reverse 5	5'TCATAATGGCAGT TTTTACCACCAATCTGTTCTCTGTGAGCCTC
<hr/>	
TapA₇₁₋₁₉₀	TapA_{71ff} C-terminus Sumo
Forward 6	5'GATAAACGCTGGGATCAAAGT GATTGACATATCAGATC
Reverse 6	5'CCAGCGTTTATCACCACCAATCTGTTCTCTGTGAGCCTC
<hr/>	
TapA₇₅₋₁₉₀	C-terminus Sumo TapA_{75ff}
Forward 7	5'AGAGAACAGATTGGTGGT GCTGATCAAAGTATTGACATATCAGATCAAACGG
Reverse 7	5'TGTGCAAATCACTTT GATCAGC ACCACCAATCTGTTCTCTGTGAGCCTCAATAATATCG

Table S6. Primers for Biofilm experiments.

Primer	Sequence	Used for
RK221	ACAT gcatgc TTATTCATCGCATTTTGCAAGCCTC	pKXD2, pKXD3, pKXD4, pKXD5
RK222	ACAT gcatgc TTA CTGATCAGCTTCATTGC	pKXD6, pKXD7
RK224	CCGATGATACAAGCGCTGCT GATCAAAGTGATTTG	pKXD3
RK225	GATATGTGCAAATCACTTTGATC AGCAGCGCTTGTATC	pKXD3
RK226	CCGATGATACAAGCGCTGCT GATAAACGCTGGGATC	pKXD4
RK227	CACTTTGATCCCAGCGTTTATC AGCAGCGCTTGTATC	pKXD4
RK228	CATTTTCAGTCTGACTGCCGCAATA GCTTTTCATGATATTG	pKXD5, pKXD6
RK229	CAAATGTTTCAATATCATGAAAAGC TATTGCGGCAGTCAG	pKXD5, pKXD6
RK234	CACAATCAGCAAAGGCGAAGCAATCAGACCAGAAGG	pKXD13
RK235	CCCGCTTTCCTTCTGGTCTGATTGCTTCGCCTTTTGCTGATTG	pKXD13
RK239	TGGCGAATTCTCAGAGTTAAATGGTATTGCTTCACT	pKXD13
RK240	GACTAGTCC TTAATTTTTATCCTCGCTATGCGC	pKXD13
RK242	TCCCCCGGGGGGATCAGAGTTAAATGGTATTGCTTCACT	pKXD2-7
RK243	GCTCTAGAGCCTCAGAGTTAAATGGTATTGCTTCACT	pKXD13
KD117	aCGTTTGAAGTGAGACATC	pKXD23
KD118	AAGCATGCAAGCTAATTC	pKXD23

Table S7. Plasmids for Biofilm experiments.

Plasmid	Genotype	Construction of strain
pKXD2	<i>pBS2E-P_{tapA}-tapA190</i>	BKD34
pKXD3	<i>pBS2E-P_{tapA}-tapA190Δ45-74</i>	BKD35
pKXD4	<i>pBS2E-P_{tapA}-tapA190Δ45-70</i>	BKD36
pKXD5	<i>pBS2E-P_{tapA}-tapA190Δ34-43</i>	BKD37
pKXD6	<i>pBS2E-P_{tapA}-tapA253Δ34-43</i>	BKD38
pKXD7	<i>pBS2E-P_{tapA}-tapA</i>	BKD39
pKXD13	<i>pBS1K-P_{tapA}-tapAΔ13-234-sipW-tasA</i>	BKD30
pKXD23	<i>pBS2E-P_{tapA}-tapA1-57</i>	BKD121

Table S8. Strains for Biofilm experiments.

Strain	Genotype	Reference
DK1042	NCIB 3610 <i>comIQ12L</i>	(4)
BRK49	<i>comIQ12L ΔtapA-sipW-tasA::spc</i>	(5)
BRK263	<i>ΔsipW::erm</i>	(5)
BKD30	<i>comIQ12L ΔtapA-sipW-tasA::spc</i> <i>amyE:: P_{tapA}-tapAΔ13-234-sipW-tasA-kan</i>	This study
BKD34	<i>comIQ12L ΔtapA-sipW-tasA::spc</i> <i>amyE:: P_{tapA}-tapAΔ13-234-sipW-tasA-kan</i> <i>lacA:: P_{tapA}-tapA190-erm</i>	This study
BKD35	<i>comIQ12L ΔtapA-sipW-tasA::spc</i> <i>amyE:: P_{tapA}-tapAΔ13-234-sipW-tasA-kan</i> <i>lacA::P_{tapA}-tapA190Δ45-74-erm</i>	This study
BKD36	<i>comIQ12L ΔtapA-sipW-tasA::spc</i> <i>amyE:: P_{tapA}-tapAΔ13-234-sipW-tasA-kan</i> <i>lacA:: P_{tapA}-tapA190Δ45-70-erm</i>	This study
BKD37	<i>comIQ12L ΔtapA-sipW-tasA::spc</i> <i>amyE:: P_{tapA}-tapAΔ13-234-sipW-tasA-kan</i> <i>lacA:: P_{tapA}-tapA190Δ34-43-erm</i>	This study
BKD38	<i>comIQ12L ΔtapA-sipW-tasA::spc</i> <i>amyE:: P_{tapA}-tapAΔ13-234-sipW-tasA-kan</i> <i>lacA:: P_{tapA}-tapAΔ34-43-erm</i>	This study
BKD39	<i>comIQ12L ΔtapA-sipW-tasA::spc</i> <i>amyE:: P_{tapA}-tapAΔ13-234-sipW-tasA-kan</i> <i>lacA:: P_{tapA}-tapA-erm</i>	This study
BKD121	<i>comIQ12L ΔtapA-sipW-tasA::spc</i> <i>amyE:: P_{tapA}-tapAΔ13-234-sipW-tasA-kan</i> <i>lacA:: P_{tapA}-tapA57-erm</i>	This study

SI References

1. C. Gille, M. Föhling, B. Weyand, T. Wieland, A. Gille, Alignment-Annotator web server: rendering and annotating sequence alignments. *Nucleic Acids Res.* **42**, W3–W6 (2014).
2. A. E. Bennett, R. G. Griffin, J. H. Ok, S. Vega, Chemical shift correlation spectroscopy in rotating solids: Radio frequency-driven dipolar recoupling and longitudinal exchange. *J. Chem. Phys.* **96**, 8624–8627 (1992).
3. A. S. Maltsev, J. Ying, A. Bax, Deuterium isotope shifts for backbone ¹H, ¹⁵N and ¹³C nuclei in intrinsically disordered protein α -synuclein. *J. Biomol. NMR* **54**, 181–191 (2012).
4. M. A. Konkol, K. M. Blair, D. B. Kearns, Plasmid-Encoded ComI Inhibits Competence in the Ancestral 3610 Strain of *Bacillus subtilis*. *J. Bacteriol.* **195**, 4085–4093 (2013).
5. R. M. Alver, “The role of ClpC and its adaptor proteins in protein quality control systems of *Bacillus subtilis*,” Hannover : Leibniz Universität Hannover. (2020) <https://doi.org/10.15488/10150> (July 18, 2022).